ABSTRACT

Title of Dissertation:	IMPACT OF SOCIAL THREAT ON EXTENDED AMYGDALA FUNCTION IN ADOLESCENT SOCIAL ANXIETY
	Rachael Mei Mei Tillman, Doctor of Philosophy, 2021
Dissertation directed by:	Professor Alexander Shackman, Psychology

Anticipation of uncertain social threat and certain-and-immediate presentation of social threat are key processes in social anxiety. Despite the public health burden of social anxiety disorder and the need to develop new treatments, the neural systems recruited during uncertain anticipation and presentation of social threat remain unclear. Further, adolescence is a period of peak vulnerability to developing more significant and persistent forms of social anxiety, but prior work has not yet examined neural substrates of both types of social threat processes during adolescence. The central extended amygdala (EAc)—including the bed nucleus of the stria terminalis (BST) and the dorsal amygdala in the region of the central nucleus (Ce)—plays a key role in prominent neuroscientific models of uncertain threat anticipation, but the relevance of these regions to social anxiety in adolescence remains poorly understood.

We examined the neural circuits engaged during the anticipation of temporally uncertain social threat and presentation of social threat in a sample of 66 adolescents enriched for clinically significant levels of social anxiety. BST and Ce reactivity was rigorously assessed and directly compared in an unbiased manner using recently developed anatomical regions of interest. Results revealed that social anxiety symptoms were

positively correlated with subjective ratings of anticipatory distress during our task, particularly during anticipation of social threat. Adolescents with heightened social anxiety showed marginally diminished EAc activation during temporally uncertain anticipation of social threat. Social anxiety symptoms were unrelated to any other brain activation elicited by the paradigm. Among all participants, increased activation was found in the EAc in response to temporally uncertain anticipation of social threat relative to certain anticipation of social threat. The EAc also showed heightened reactivity during presentation of social threat relative to presentation of benign social stimuli. Exploratory whole-brain voxelwise analyses highlighted a widely distributed network of regions previously implicated in social cognitive processes and the expression and regulation of fear and anxiety. Taken together, these observations hint at a potentially unique role of the EAc in social anxiety in adolescence and provide support that the EAc makes broadly similar contributions to governing responses to social threat.

IMPACT OF SOCIAL THREAT ON EXTENDED AMYGDALA FUNCTION IN ADOLESCENT SOCIAL ANXIETY

by

Rachael Mei Mei Tillman

Dissertation submitted to the Faculty of the Graduate School of the
University of Maryland, College Park, in partial fulfillment
of the requirements for the degree of
Doctor of Philosophy
2021

Advisory Committee:
Professor Alexander Shackman, Chair
Professor Andres De Los Reyes
Professor Jack Blanchard
Associate Professor Tracy Riggins
Professor Nathan Fox, Dean's Representative

Acknowledgements

I am deeply grateful to the participants and their families who contributed to this research. I also would like to thank my advisor, Dr. Alex Shackman, for his support, teaching, and mentoring throughout this project and my PhD journey. Further, I am extremely fortunate to have had the support, training, and friendship of my fellow lab members including senior staff, graduate student colleagues, and research assistants. In particular, thank you to Allegra Anderson, Samiha Islam, Gloria Kim, Shannon Grogans, Dr. Jason Smith, and Kathryn DeYoung – the completion of this project would not have been possible without you all! I am also grateful to the Maryland Neuroimaging Center staff for their assistance during data collection. Lastly, I have tremendous gratitude for my family and friends and their constant support throughout this long process. Special thanks to my husband, Ben Stephenson, and my brother, Zachary Tillman, who provided so much encouragement, lots of laughs, and were always willing to help me talk through challenges.

Table of Contents

List of Tables

List of Figures

Chapter 1: Introduction

Background

Social anxiety is characterized by fear and anxiety related to evaluation from others. Like other anxieties, social anxiety is widely conceptualized as a dimensional construct, ranging from momentary discomfort in acute performance situations to debilitating illness (Bögels et al., 2010; Conway et al., 2019; Merikangas, Avenevoli, Acharyya, Zhang, & Angst, 2002; Schneier et al., 2002). Social anxiety becomes pathological when these symptoms or the distress caused by them chronically impair function (American Psychiatric Association, 2013). Social anxiety disorder (SAD) is among the more common psychiatric illnesses, with an estimated lifetime prevalence of 6-13% (Angst et al., 2016; Bandelow & Michaelis, 2015; Kessler et al., 2012). Onset of the disorder typically occurs early in development and persists into adulthood (Heimberg et al., 2014; Cartwright-Hatton et al., 2006).

Adolescence marks a period of peak vulnerability for SAD, with 75% of severe cases first emerging by mid-adolescence (Gregory et al., 2007; Haller, Kadosh, Scerif, & Lau, 2015; Kessler et al., 2005, 2012). Normative changes across multiple levels (e.g., biological changes related to puberty, environmental transitions related to schooling) during the adolescence period are thought to confer unique vulnerability for the development and maintenance of SAD (Caouette & Guyer, 2014; Leigh & Clark, 2018). These changes, which include an increase in public self-consciousness, heightened emotional salience of peer interactions, and susceptibility to peer influence, are thought to foster the emergence and persistence of social fears for some adolescents (Caouette &

Guyer, 2014; Eldreth et al., 2013; Leigh & Clark, 2018). SAD often has deleterious consequences for academic achievement, social function, and wellbeing and can contribute to the development of co-morbid psychiatric and physical illnesses (Beesdo-Baum & Knappe, 2012; Ezpeleta et al., 2001 Stein et al., 2017). Existing treatments are challenging to access, costly, and ineffective for many youth, underscoring the need to develop a deeper understanding of the neural systems governing the expression of adolescent SAD (James et al., 2013; Knight et al., 2014; Craske et al., 2017).

Paralleling other anxiety disorders, SAD is characterized by pathological fear and anxiety in two kinds of situations: (1) When social threat is certain-and-immediately present, as when conversing with unfamiliar individuals in a group, and (2) when social threat is uncertain-and-remote but anticipated, that is, situations where social threat is possible, but the precise timing or likelihood is unclear (e.g., upon entering a store or a classroom; American Psychiatric Association, 2013; Grupe & Nitschke, 2013; Davis et al., 2010). Both facets are important, but a growing body of evidence suggests that exaggerated and excessive anticipatory responding under conditions of threat uncertainty is especially relevant for the development and maintenance of anxiety disorders (Abend et al., 2020; Craske et al., 2012; Duits et al., 2015; Grupe & Nitschke, 2013). In the context of SAD, apprehension about social and evaluative situations—which are often dynamic and challenging to predict—can reinforce avoidance and safety behaviors. These behaviors can, in turn, increase maladaptive appraisals of social and evaluative situations (e.g., overestimating negative consequences of a social encounter, believing one's social skills to be poor; Hofmann, 2007). Adolescence in particular is associated with weaker and more fluid self-concept, providing a critical window in which maladaptive cognitive biases and

beliefs about one's self and about the social world can take root and lead to more negative social-emotional outcomes (for a review, see Rappee et al., 2019).

Central Extended Amygdala and Anxiety

Evidence gleaned from animal models and human neuroimaging work highlights the role of the central extended amygdala (EAc) in the two facets of anxiety disorders, certain-and-immediate presentation of threat and uncertain-and-remote anticipation of threat (Fox & Shackman, 2019), suggesting EAc involvement in the parallel *social* threat processes that characterize extreme social anxiety. The EAc encompasses a tightly interconnected group of subcortical regions characterized by similar cytoarchitecture, neurochemistry, and gene expression (Alheid & Heimer, 1988; Fox, Oler, Tromp, Fudge, & Kalin, 2015; Oler et al., 2017; Yilmazer-Hanke, 2012). Two specific regions of the EAc, the dorsal amygdala in the region of the central nucleus (Ce) and the lateral division of the neighboring bed nucleus of the stria terminalis (BST), are particularly implicated in the neurobiology of threat processing. While existing research has not yet directly explored EAc functioning related to *social* threat presentation and anticipation during *human adolescence*, emerging work has begun to target the EAc in anticipatory responding to threat among adults. The below section serves as a brief review of hypotheses related to EAc function.

Based on earlier perturbation studies in rodents (e.g., Davis, 2006), clinicians and neuroimagers have come to widely believe that the amygdala triggers responses to certain-and-immediate threat, whereas the BST triggers responses to uncertain-and-remote threat anticipation (e.g., Sylvers et al., 2011; Somerville et al., 2010, 2013; LeDoux & Pine 2016; Klumpers et al., 2017). Indeed, this hypothesis has even been incorporated into the National

Institute of Mental Health's influential Research Domain Criteria (RDoC) framework (National Institute of Mental Health, 2011, 2020 a, b). Consistent with this hypothesis, several human neuroimaging studies provide evidence that the Ce is sensitive to threat that is clear, present, and immediate, and the BST is sensitive to sustained response to threat that is distal and uncertain (Alvarez, Chen, Bodurka, Kaplan, & Grillon, 2011; Brinkmann et al., 2017; Somerville et al., 2010, 2013; Herrmann et al., 2016; Avery, Clauss, Blackford, 2016; Münsterkötter et al., 2015). For example, Somerville and colleagues (2010) presented either aversive or neutral images (3 seconds) in relatively long blocks (118-sec) where the timing of image presentations was either certain or uncertain. This task allowed comparison of both immediate and clear threat presentation (i.e., aversive images) and uncertain anticipation responses (i.e., long anticipation blocks preceding delivery of images) in the same individuals. Analyses revealed activation in the amygdala in response to the negative images and activation in the BST during negative anticipation blocks versus neutral and uncertain anticipation blocks versus certain anticipation blocks, lending support for the "double-dissociation" account. Further, this work suggests that the BST is more responsive to threat anticipation among individuals with a more anxious disposition or an anxiety disorder (Somerville, Whalen, & Kelley, 2010, Yassa, Hazlett, Stark, & Hoehn-Saric, 2012; Münsterkötter et al., 2015). Collectively, this body of work aligns with the functional "double-dissociation" hypothesis, which posits that the Ce and BST orchestrate responses to distinct kinds of threat and thus are functionally dissociable.

However, a growing body of perturbation and recording work in rodents and human neuroimaging studies contradict this "double dissociation" account (Shackman & Fox, 2016; Fox & Shackman, 2019; Hur et al., 2020). Mechanistic studies in rodents

demonstrate that defensive responses to uncertain-and-remote threat are assembled by microcircuits encompassing both the Ce and BST (Gungor and Paré, 2016; Lange et al., 2017; Ahrens et al., 2018; Ressler et al., 2020). This work motivates the competing hypothesis that the Ce and the BST, while certainly not interchangeable, are more functionally alike than different, and that they work together to trigger defensive responses to both certain-and-immediate *and* uncertain-and-remote threats (Shackman and Fox, 2016; Fox and Shackman, 2019). Findings from human imaging work support this "integration" hypothesis. Studies have reported elevated dorsal amygdala (Ce) activation during the anticipation of uncertain threat (Williams et al., 2015; Andreatta et al., 2015; Lieberman, Gorka, Shankman, & Phan, 2017), heightened responses in both the BST and the region of the dorsal amygdala (Ce) while anticipating uncertain threat (Mobbs et al., 2010), and activation of the BST in response to brief, predictive cues, indicating sensitivity to certain threat (Klumpers et al., 2015). Most recently, Hur et al. (2020) demonstrated that the Ce and BST showed statistically indistinguishable activation during the anticipation of temporally uncertain and certain noxious stimuli, reinforcing the hypothesis that they make broadly similar contributions to governing responses to threat.

Functional Neuroimaging Work in Social Anxiety

In the context of social anxiety, certain-and-immediate and uncertain-and-remote *social* threat processes have typically been investigated separately and few studies have specifically interrogated the EAc. In this section, I briefly review the existing body of neuroimaging work.

Certain-and-Immediate Threat Presentation

To date, the vast majority of functional neuroimaging studies of social anxiety have focused on certain-and-immediate presentation of social threat. Paradigms used in these studies are designed to mimic acute social threat and include evaluative contexts and threat-related social cues (e.g., angry faces or voices; Miskovic & Schmidt, 2012; Gentili et al., 2016; Cremers & Roelofs, 2016; Brühl, Delsignore, Komossa, & Weidt, 2014; Jarcho et al., 2013; Heitmann et al., 2017). A meta-analysis encompassing 40 studies of adult SAD indicated elevated reactivity to immediate social threat in a number of regions, including the amygdala, insula, anterior cingulate cortex (ACC), and specific regions within the prefrontal cortex (PFC), including medial (mPFC) and dorsolateral prefrontal cortex (dlPFC) (Brühl et al., 2014). Likewise, a meta-analysis of 23 studies of face perception in predominantly adult SAD samples (1 study assessed adolescents) indicated increased engagement in the amygdala, ACC, PFC, and superior temporal sulcus (STS) (Gentili et al., 2016). A broadly similar pattern is evident among adults with elevated dispositional shyness and social anxiety (Pujol et al., 2009; Carré et al., 2014; Beaton et al., 2010). Findings in pediatric SAD or in children and adolescents at risk for developing SAD also show a generally similar pattern in response to simple social cues and more complex situations of social-evaluative threat (for a review, see Jarcho et al., 2013). That is, differential involvement of similar regions—including heightened amygdala reactivity and alterations in circuits encompassing mPFC and ventral lateral prefrontal cortex (vlPFC), insula, and ACC—is hypothesized to work together to detect certain-and-immediate social threat cues, ascribe salience, and assemble defensive responses.

Uncertain-and-Remote Threat Anticipation

Much less scientific attention has been dedicated to characterizing the neural systems underlying exaggerated reactivity to uncertain-and-remote social threat. In fact, only a handful of functional neuroimaging studies have examined anticipation of social threat in social anxiety (Tillfors et al., 2002; Lorberbaum et al., 2004; Boehme et al., 2014; Davies et al., 2017, Figel et al., 2019, Clauss et al., 2019).

In a pioneering positron emission tomography study, Tillfors et al. (2002) demonstrated that adults with SAD show enhanced blood flow in the posterior amygdala, anterior hippocampus, and dorsolateral prefrontal and inferior temporal cortices while preparing to give an "evaluated" speech. Consistent with this, Lorberbaum et al. (2004) and Boehme et al. (2014) used functional MRI (fMRI), to demonstrate that adults with SAD show increased activation in the amygdala and insula during speech anticipation. Davies et al. (2017) assessed time course and magnitude of neural engagement of the amygdala during speech anticipation and found the time course of amygdala activity was more prolonged and less variable among adult SAD patients.

EAc in Social Anxiety

To date, only two studies have specifically examined the contribution of the EAc to uncertain-and-remote threat anticipation in social anxiety. Figel et al. (2019) manipulated social evaluation using a video camera observation task and a case-control design (n=22 SAD adult patients and 23 health controls*)*. At the start of each trial, a cue indicated whether (aversive trials) or not (benign trials) their face would be recorded by a video camera positioned on the scanner head coil. Cues were followed by an anticipation period of variable and unsignaled duration, which terminated with a second cue indicating whether or not the camera was recording. An a priori anatomical region-of-interest (ROI)

approach was used to rigorously assess Ce and BST activation during each phase of the trial. Results revealed that adults with SAD showed significantly increased activation to the certain-and-immediate recording cue in both the Ce and the BST. In contrast, both SAD patients and healthy controls similarly elevated BST activation during the period of uncertain-and-remote anticipation.

Clauss et al. (2019) used an uncertain "threat-of-faces" and a dimensional approach utilizing selective recruitment strategies to enrich their participant sample for high social anxiety (n=44 adults). On certain threat trials, a brief cue (1 second) signaled the certain presentation (p=1.00) of a fearful face. On certain safety trials, a second cue signaled the certain presentation (p=1.00) of a neutral face. On uncertain threat trials, a third cue signaled the uncertain presentation (p=0.50) of a fearful face. An a priori anatomical region-of-interest (ROI) approach was also used to rigorously assess amygdala and BST activation during each of the cues and actual presentation of face stimuli. Results revealed that adults with higher levels of social anxiety showed heightened BST activation relative to amygdala during the unpredictably signaled presentation of threat-related (fearful) faces compared to neutral faces.

While these findings provide some crucial preliminary insights into the neural substrates of uncertain anticipation in social anxiety, there are some important limitations to prior work. To our knowledge, existing work has not yet examined the neural underpinnings of anticipation in youth with heightened social anxiety[1]. Extending current

[1] This has been investigated in studies focused on mixed pediatric anxiety disorders and in youth at-risk for developing SAD (Guyer et al., 2008, 2009; Spielberg et al., 2015; Smith et al., 2020) and provides important insights into social anxiety in youth during more ecologically valid states of anticipation. These studies have demonstrated that youth with anxiety disorders exhibited increased activation in the amygdala relative to non-anxious youth when anticipating feedback from peers the participants had previously rejected relative to peers the participants had previously selected (Guyer et al., 2008, 2009; Spielberg et al., 2015). These findings were not observed in youth at-risk for developing SAD. While findings are

accounts of EAc function and threat anticipation to adolescence could determine whether insights gleaned from adults translate to this developmental period. Some prior work has also failed to provide behavioral evidence that their tasks elicit anxiety within their current participant sample (Clauss et al., 2019). Further, existing studies have not yet directly compared uncertain to certain threat anticipation in social anxiety, precluding more complete accounts of the role of uncertainty independent of valence in models of social anxiety.

Current Study

To address these questions, we combined fMRI with the Maryland Social Threat Countdown (MSTC) task in an adolescent sample enriched for clinically significant levels of social anxiety. Traditional case-control studies are limited by arbitrary boundaries, inadequate reliability, and marked heterogeneity, impeding clinical utility and neurobiological discovery (Cuthbert & Insel, 2010; 2013; Hur, Tillman, Fox, & Shackman, 2019; Kotov et al., 2017; Latzman et al., 2020). To overcome this barrier, we used a targeted recruitment strategy to capture a broad range of social anxiety symptoms and a dimensionally focused, RDoC-style analytic framework to rigorously interrogate the impact of social anxiety on the neural systems responsive to uncertain-and-remote and certain-and-imminent social threat.

Building on prior work from our group (Hur et al., 2020) and others (Somerville et al., 2010, 2013; Grupe et al., 2016; Pedersen et al., 2019), the MSTC paradigm is an fMRI-

conceptually significant, it is unclear whether either condition (anticipation of feedback from previously rejected peers *or* anticipation of feedback from previously accepted peers) adequately represents the uncertain anticipation of an emotionally neutral outcome. Further, literature on fear of positive evaluation demonstrates this concept uniquely contributes to SAD (for a review, see Fredrick & Luebbe, 2020) suggesting that anticipation of feedback from previously accepted peers may not adequately serve as a control condition.

optimized version of temporally uncertain-threat assays that have been validated using fear-potentiated startle and acute anxiolytic administration (e.g., benzodiazepine) in mice (Daldrup et al., 2015; Lange et al., 2017), rats (Miles et al., 2011), and humans (Hefner et al., 2013), enhancing its translational relevance (**Figure 1**). The MSTC paradigm takes the form of a 2 (*Valence:* Threat/Safety) × 2 (*Temporal Certainty:* Uncertain/Certain) × 2 (*Period:* Anticipation/Presentation) randomized event-related design (3 scans; 6 trials per condition; 4 conditions per scan). On Certain Threat trials, participants saw a descending stream of integers ("count-down"; e.g., 30, 29, 28...3, 2, 1) for 18.75 seconds. This anticipation period always culminated with the presentation period, the delivery of a socially threatening photograph (angry face) and audio clip (e.g., *"No one wants you here"*). Uncertain Threat trials were similar, but the integer stream was randomized and presented for an uncertain and variable duration (8.75-32.50 seconds; *M*=18.75 seconds). Here, subjects knew that social threat was going to be delivered, but they had no way of knowing precisely *when* it would occur. Safety trials were similar but terminated with the delivery of comparatively benign photographs (happy face) and audio clips (*"I play soccer"*). Valence was continuously signaled during the anticipation period by the background color of the display.

Recently developed anatomical ROIs made it possible to rigorously assess and directly compare Ce and BST reactivity in an unbiased manner (Poldrack et al., 2017). This approach allowed us to adjudicate between the "double dissociation" and "integration" hypotheses. The "double dissociation" hypothesis suggests that the acute presentation of social threat will recruit the Ce, the uncertain anticipation of social threat will recruit the BST, and this pattern will be amplified among adolescents with more severe social anxiety.

In contrast, the "integration" hypothesis suggests that both regions are recruited to a similar degree by the presentation of social threat and the uncertain and certain anticipation of social threat, and that this pattern will be exaggerated among more socially anxious adolescents. This approach also allowed us to determine whether insights gleaned from studies in adults with social anxiety extend to adolescents (Clauss et al., 2019; Figel et al., 2019). A series of whole-brain voxelwise analyses allowed us to explore associations between social anxiety severity and activation of cortical regions (e.g., insula, ACC, dlPFC) implicated in adults with SAD (Miskovic & Schmidt, 2012; Gentili et al., 2016; Cremers & Roelofs, 2016; Brühl, Delsignore, Komossa, & Weidt, 2014; Heitmann et al., 2017) and youth with social anxiety (Jarcho et al., 2013).

Chapter 2: Method

Study Overview

Following preliminary online and telephone screening (see below), eligible individuals completed a combined clinical and laboratory session that encompassed informed written consent and adolescent assent, self-report assessments, a structured clinical assessment (see below), and an MRI assessment. Prior to scanning, participants practiced the fMRI paradigm until staff confirmed understanding. All procedures were approved by the University of Maryland Institutional Review Board.

Participants

Eighty-four participants between the ages of 13-17 years old and their parents were recruited from advertisements distributed online (i.e., Facebook, listservs), flyers posted at community mental health clinics and broader community settings (i.e., coffee shops, local community centers), and referrals from other university research studies recruiting adolescents. Advertisements were designed to differentially target adolescents with high social anxiety using language inviting "shy" or "socially anxious" adolescents to participate in a study about brain function. Advertisements designed for adolescents without high levels of social anxiety used general language to invite participants to enroll, such as "Are you a teen?" or "Have a teen aged 13-17?", and these advertisements were only distributed in general settings and not in mental health clinics.

To ensure inclusion of a clinically enriched sample that comprised both adolescents with social anxiety disorder and adolescents with low levels of social anxiety, participants completed a preliminary screening questionnaire online. The preliminary screening included a measure of the frequency of social anxiety disorder symptoms (the abbreviated

Social Phobia and Anxiety Scale for Children; SPAIC-11; Bunnell, Beidel, Liu, Joseph, & Higa-McMillan, 2015) and three additional questions designed to assess interference and distress from social anxiety symptoms using a 5-point Likert scale (*1 = Not at all, 5 = Extremely*; See Appendix for questions). Individuals were invited to enroll if they met *any* of the following preliminary inclusion criteria: 1) obtaining a score of 16 or above on the SPAIC-11 (Bunnell et al., 2015); 2) indicating social anxiety interference or distress on the online screener prior to enrollment; and 3) obtaining a score of 6 or below on the abbreviated SPAIC-11 (Bunnell et al., 2015) *and* indicating low social anxiety interference and distress on the online screener prior to enrollment.

For additional enrollment criteria, participants in both groups were native English speakers, right-handed, had no history of head injury, seizures, or any other characteristics that would prevent MRI scanning (metal or electronics in the body, including metal plates or joints, orthodontics, and surgical staples; claustrophobia; inability to lie still for extended periods). Exclusionary criteria for both groups were the presence or history of psychosis, autism spectrum disorder, bipolar disorder, or psychiatric medication used for treating anxiety or depression (e.g., selective-serotonin reuptake inhibitors, benzodiazepines, buspirone, tricyclics, monoamine oxidase inhibitors).

Eighteen participants were excluded from analyses due to the following reasons: premature termination of scanning (n=3), insufficient in-scanner behavioral responses (<50% completed assessments; n=3), significant motion artifact (n=6), and significant disparity between time of SPAIC-11 assessment and time of scan (n=6). The final sample included 66 adolescents (60.6% female; 50% White, 6.1% Asian, 30.3% Black, 6.1% multiracial/other, and 7.6% Hispanic) who endorsed a broad spectrum of social anxiety

symptom severity: 36.3% adolescents (male n=10) with high social anxiety who met criteria for a DSM-IV SAD diagnosis, as assessed via clinical interview, 22.7% adolescents (male n=2) with intermediate social anxiety as defined by SPAIC-11 scores greater than 6 that did not meet criteria for a SAD diagnosis, and 40.9% adolescents (male n=14) with low social anxiety as defined by SPAIC-11 scores at 6 or lower. All participants were free from psychotropic medication at the time of the MRI assessment. Adolescents with low social anxiety were free of lifetime internalizing psychiatric disorders. The mean age was 15.37 years old (standard deviation=1.32; range=13.18-17.99).

Measures

Social Phobia and Anxiety Scale for Children

The SPAIC-11 was administered at two time points during the course of study: 1) prior to enrollment as a screening measure and 2) after enrollment during the participant's study visit as a measure of current anxiety symptomology. The SPAIC-11 was developed as a brief version of the 26-item Social Phobia and Anxiety Inventory using item response theory (Bunnell et al., 2015). Items on the SPAIC-11 describe social situations, and the respondent endorses how often they feel nervous or scared in that situation (e.g., "I feel scared when I have to speak or read in front of a group of people"). The three response choices range from 0 (Never) to 2 (Always). Total scores range from 0 to 22, with higher scores reflecting higher levels of social anxiety. The SPAIC-11 showed adequate sensitivity and specificity and reliably differentiated between youth with and without a social anxiety disorder diagnosis (Bunnell et al., 2015). The measure demonstrated good internal consistency (Cronbach's α=0.90; Bunnell et al., 2015).

SPAIC-11 scores used in the dimensional analysis were those collected on the scan date, with the exception of 7 scores which were collected prior to the scan at the screening date. Of these 7 scores, average time from screening to scan was 30 days. Age and mean-centered SPAIC-11 score were not correlated (r=0.15, p=0.22). Analysis of sex and racial demographic differences in SPAIC-11 scores are presented in **Table 1**. Males and females did not significantly differ in levels of social anxiety. White/European American participants and Black/African American, Asian, Multiracial, and other participants that did not identify as White/European American did not significantly differ in levels of social anxiety.

Pubertal Development Scale

To evaluate whether social anxiety symptoms were related to pubertal development, adolescents' pubertal status was measured using the self-reported Pubertal Development Scale (PDS; Petersen, Crockett, Richards, & Boxer, 1988). Items from this scale reflect areas of pubertal development for females' and males', such as growth, adrenal, and gonadal development. Males were asked whether they had noticed the start of pubic hair growth, underarm hair growth, facial hair growth, acne, and voice change. Females were asked whether they had noticed the start of pubic hair growth, underarm hair growth, acne, and breast development and whether menarche had occurred. The final item asked adolescents to assess the timing of their development in relation to their same-age peers. The response choices ranged from 1 (development not yet started) to 4 (development complete). Scores were averaged to make a composite score, with higher scores reflecting higher levels of physical maturation. In the current sample, 3 participants did not have PDS data. The PDS has been found to be a robust measure of pubertal development with high

correlations with pubertal clinical exams rated by healthcare professionals (r=0.82 – 0.86 for agreement within one pubertal development stage between self-report PDS and healthcare professional exams; Schmitz, Hovell, Nichols, Irvin, Keating, Simon, et al., 2004; Shirtcliff, Dahl, & Pollak, 2009). The measure demonstrated acceptable internal consistency (Cronbach's α=0.68 – 0.83; Petersen et al., 1988; Carskadon & Acebo, 1993). SPAIC-11 and PDS were unrelated (p=0.94).

Mini-International Neuropsychiatric Interview for Children and Adolescents

Diagnostic status was assessed by a masters-student level clinician using modules from the Mini-International Neuropsychiatric Interview for Children and Adolescents (MINI-KID; Sheehan et al., 1998). The MINI-KID is a structured diagnostic interview for children aged between 6 and 17 years old based on DSM-IV and ICD-10 criteria. The MINI-KID has good concordance with gold-standard diagnostic measures (i.e., the Kiddie Schedule for Affective Disorders and Schizophrenia- present and lifetime version; Kaufman et al., 1997), good test-retest reliability, and discriminates individuals with social anxiety from healthy individuals, as well as differentiates between social anxiety disorder from other anxiety disorders (Sheehan et al., 2010). The following modules were administered to adolescent participants: Depression, Dysthymia, Panic Disorder, Separation Anxiety Disorder, Social Anxiety Disorder, Specific Phobia, Post-Traumatic Stress Disorder (PTSD), Attention Deficit/Hyperactivity Disorder (ADHD) and Generalized Anxiety Disorder (GAD). Interviews were completed one-on-one (i.e., without the parent present) to encourage frank reporting. See Appendix for detailed diagnostic breakdown of participants.

Procedure

Paradigm Structure and Design Considerations

The MSTC paradigm takes the form of a 2 (*Valence:* Threat/Safety) × 2 (*Temporal Certainty:* Uncertain/Certain) × 2 (*Period:* Anticipation/Presentation) randomized event-related design (3 scans; 6 trials per condition; 4 conditions per scan). Simulations were used to optimize the detection and deconvolution of task-related hemodynamic signals (variance inflation factors <1.68). Stimulus presentation and ratings acquisition were controlled using Presentation software (version 19.0, Neurobehavioral Systems, Berkeley, CA).

On Certain Threat trials, subjects saw a descending stream of integers ("count-down"; e.g., 30, 29, 28...3, 2, 1) for 18.75 seconds. To ensure robust social anxiety, this anticipation epoch always culminated with the delivery of a socially threatening photograph (angry face) and audio clip (e.g., *"No one wants you here"*). Uncertain Threat trials were similar, but the integer stream was randomized and presented for an uncertain and variable duration (8.75-32.50 seconds; *M*=18.75 seconds). Here, subjects knew that something aversive was going to occur, but they had no way of knowing precisely when it would occur. Consistent with recent recommendations (Shackman and Fox, 2016), the average duration of the anticipatory epoch was identical across conditions, ensuring an equal number of measurements (TRs/condition). Mean duration was chosen to enhance detection of task-related differences in the blood oxygen level-dependent (BOLD) signal (Henson, 2007), and to enable dissection of onset from genuinely sustained responses. Safety trials were similar but terminated with the delivery of comparatively benign photographs (happy face) and audio clips (*"I play soccer"*). Valence was continuously

signaled during the anticipatory epoch by the background color of the display. Temporal certainty was signaled by the nature of the integer stream. Certain trials always began with the presentation of the number 30 (**Figure 1**). On Uncertain trials, integers were randomly drawn from a near-uniform distribution ranging from 1 to 45 to reinforce the impression that Uncertain trials could be much longer than Certain ones and to minimize incidental temporal learning ("time-keeping"). White-noise visual masks (3.2 seconds) were presented between trials to minimize persistence of the visual reinforcers in iconic memory. Subjects provided ratings of anticipatory anxiety for each trial type during each scan using an MRI-compatible response pad (MRA, Washington, PA; **Figure 1**). Subjects were instructed to rate the intensity of anxiety experienced during the prior anticipation ("countdown") period using a 1-4 (*least/most*) scale. Subjects were prompted to rate each trial type once per scan. A total of 6 additional echo-planar imaging (EPI) volumes were acquired at the beginning and end of each scan (see below).

Prior to entering the scanner, participants completed a practice version of the paradigm while sitting at a desktop computer. The practice version guided participants through each type of condition with examples and required participants to complete an anxiety rating with a response pad identical to the device used in the scanner. At the end of the practice version of the MSTC, participants were queried about specific elements of the task to ensure understanding (e.g., the meaning of the ratings, the types of conditions). After entering the scanner and completing preparatory scans, instructions from the practice version of the paradigm were repeated for all participants immediately prior to the start of the MSTC task. Verbatim instructions in the practice version of the MSTC task are detailed in the Appendix.

Visual Stimuli. Face photographs (1.8 seconds) and other visual stimuli were digitally back-projected (Powerlite Pro G5550, Epson America, Inc., Long Beach, CA) onto a semi-opaque screen mounted at the head-end of the scanner bore and viewed using a mirror mounted on the head-coil. A total of 72 face photographs were drawn from the Chicago Face Database Versions 1 and 2 (Ma, Correll, & Wittenbrink, 2015). Stimuli included 36 young-adult models of varying race and sex, each depicting 1 angry and 1 happy expression.

Auditory Stimuli. Auditory stimuli (1.8 seconds) were delivered using an amplifier (PA-1 Whirlwind) with in-line noise-reducing filters and ear buds (S14; Sensimetrics, Gloucester, MA) fitted with noise-reducing ear plugs (Hearing Components, Inc., St. Paul, MN). A total of 72 custom auditory stimuli were created by recording 36 young-adult voice actors, recruited to match the race and sex of the photograph models (see above). Each voice actor provided 1 threatening and 1 benign audio statement, equated for number of syllables. Voice actors were carefully coached to deliver the threatening statements (e.g., *"I don't like you"*) in a hostile manner and to deliver the comparatively benign statements (e.g., *"Today is nice"*) in a neutral or mildly positive manner. Audio stimuli were volume standardized. To reinforce the naturalistic nature of the paradigm, each photograph was consistently paired with a specific sex- and race-matched voice actor.

MRI Data Acquisition

MRI data were acquired using a Siemens Magnetom TIM Trio 3 Tesla scanner (32-channel head-coil). Foam inserts were used to immobilize the participant's head within the head-coil and mitigate potential motion artifacts. Subjects were continuously monitored from the control room using an MRI-compatible eye-tracker (Eyelink 1000; SR Research,

Ottawa, Ontario, Canada). Head motion was monitored using the AFNI real-time plugin (Cox, 1996). Sagittal T1-weighted anatomical images were acquired using a magnetization prepared rapid acquisition gradient echo (MPRAGE) sequence (TR = 1900 ms; TE = 2.32 ms; inversion time = 900 ms; flip angle = 9°; sagittal slice thickness = 0.9 mm; voxel size in plane = 0.449 × 0.449mm; matrix = 512 × 512; field of view = 230 × 230).

To enhance resolution, a multi-band sequence was used to collect oblique-axial echo planar imaging (EPI) volumes during the social threat anticipation task (multiband acceleration = 6; TR = 1000 ms; TE = 39.4 ms; flip angle = 36.4°; slice thickness = 2.2 mm, number of slices = 66; in-plane resolution = 2.1875 × 2.1875 mm; matrix = 96 × 96). Images were collected in the oblique axial plane (approximately −20° relative to the AC-PC plane) to minimize potential susceptibility artifacts. A total of three 568-volume scans were acquired. The scanner automatically discarded 7 volumes prior to the first recorded volume. To enable field map distortion correction, a pair of oblique-axial co-planar spin echo images with opposing phase encoding direction was acquired (TR = 7220 ms; TE = 73 ms; slice thickness = 2.2 mm; matrix = 96 × 96).

MRI Data Preprocessing

T1-weighted images were inhomogeneity-corrected with N4 (Tustison et al., 2010) and filtered using the *DenoiseImage* function in ANTS with the default Gaussian noise model (Avants et al., 2011). The full head images were then normalized to the 1-mm MNI152 template using the diffeomorphic approach implemented in SyN (Klein et al., 2009; Avants et al., 2011) then the brains were extracted using a modified version of BEaST (Eskildsen et al 2012) with normalized brains from the IXI database ((https://brain-development.org/ixi-dataset) as a reference set and the resulting probabilistic brain mask

unwarped back to native space, thresholded at 0.5, and applied. The extracted brains were then renormalized to the brain extracted MNI template, again using SyN, with the full head transforms as initialization for speed. The native space brain-extracted T1 images were also segmented using FAST (FSL version 5.0.9) (Zhang et al., 2001) and unwarped tissue priors (Lorio et al., 2016). The white matter compartment was saved for use in T1-EPI coregistration (see below) as were fieldmap and intensity images created from a single standard Siemens two TE fieldmap sequence using *fsl_prepare_fieldmap*.

With regard to functional data processing, the first 3 volumes of each EPI scan were removed, and the remaining volumes were de-spiked and slice-time corrected using AFNI (Cox, 1996). The first remaining volumes of each EPI series were coregistered to the anatomical T1 weighted images using the boundary-based registration approach with fieldmap correction implemented in FSL (Greve & Fischl, 2009). Because of miss-alignment between the fieldmap locations and the EPI data, additional nonlinear coregistration between the T1 and EPI images as well as their intensity gradients was performed with *antsRegistrationSyNQuick.sh* with the mutual information cost function. The FSL EPI to T1 affine transform and fieldmap shift image were converted to ITK format (Insight Segmentation and Registration Toolkit; Yoo et al., 2002) using *c3d* and custom software. The coregistered first EPI volumes were transformed into MNI space using the brain extracted transforms and warps and averaged across subjects and runs to create a study specific EPI template and warps to this template estimated for each image again using SyN. To minimize spatial blurring, the transformation matrices and warps for affine motion correction, affine, fieldmap shift, and nonlinear co-registration, affine and nonlinear T1 based spatial normalization to the MNI152 template, and affine and nonlinear spatial

normalization to the study specific template were concatenated and applied to the EPI data in a single step. The resulting EPI data were resampled to 2-mm isotropic voxels using 5th order splines and smoothed (6 mm FWHM). To attenuate physiological noise, white matter (WM) and cerebrospinal fluid (CSF) time-series were extracted from the spatially unsmoothed, normalized EPI data. WM and CSF compartments were identified using eroded versions of the probabilistic segmented images provided with the MNI152 template.

All datasets were visually inspected for quality assurance. To assess residual motion artifact, the number of times the brain showed a volume-to-volume displacement > 0.5 mm using the motion-corrected EPI data was computed. Scans with extreme motion variance (≥ 2.5 SDs about the mean) were excluded from analyses. To assess task-correlated motion, we computed correlations between the design matrix and the motion estimates (see above). Scans showing extreme correlations (≥ 2.5 SD) were discarded. As noted above, scans in which ≥ 50% of the behavioral responses were missed were also excluded from analyses. Participants were removed from analyses if they produced fewer than two usable scans. On this basis, nine subjects had insufficient usable data and were excluded from analyses, while 14 subjects with 2 usable scans were retained.

fMRI Modeling

fMRI data were modeled using SPM12 (https://www.fil.ion.ucl.ac. uk/spm) and in-house MATLAB code. At the first level (single-subject), the MSTC task was modeled using variable duration rectangular (boxcar) regressors time-locked to the anticipatory periods of the Uncertain Threat, Certain Threat, and Uncertain Safety trials. The anticipatory periods of Certain Safety were treated as an unmodeled, implicit baseline. Uncertain Threat, Certain Threat, Uncertain Safety, and Certain Safety reinforcer trials (in

which face/voice stimuli pairs were presented) were also modeled as event-related predictors. All predictors were convolved with a canonical HRF and its temporal derivative. Nuisance variates included volume-to-volume displacement and motion parameters (including 1st lagged version), CSF time-series, instantaneous pulse and respiration rates, and their estimated effect on the BOLD time-series. ICA-AROMA (Pruim et al., 2015) was used to model several other potential sources of noise (brain edge, CSF-edge, white matter). These and the single ICA component showing the strongest correlation with motion estimates were included as additional nuisance variates. EPI volumes with excessive volume-to volume displacement (0.33 mm), as well as those during the delivery of reinforcers, were censored.

Analytic Strategy

As a precursor to hypothesis testing, we first determined whether variation in social anxiety symptoms (SPAIC-11) influenced the intensity of anticipatory anxiety elicited by the MSTC task. This was implemented in SPSS (version 27; IBM) using a standard mixed-effects general linear model (GLM) incorporating Valence (Threat/Safety), Temporal Certainty (Uncertain/Certain), and mean-centered social anxiety (SPAIC-11). Significant interactions were decomposed using simple effects.

Our primary objective was to adjudicate between competing hypotheses regarding the role of the EAc in threat processing, the "double dissociation" and "integration" hypotheses. Using recently developed anatomical ROIs (**Figure 2**), we extracted and averaged standardized contrast coefficients for each of the relevant contrasts, separately for each ROI, in order to rigorously assess and directly compare Ce and BST reactivity in an unbiased manner. Contrasts relevant to examining competing hypotheses included each

condition (e.g., Uncertain Threat Anticipation, Uncertain Threat Presentation, Certain Threat Anticipation, etc.) compared to the implicit baseline (Certain Safety Anticipation), for both regions during anticipation periods and presentation periods. Mixed effects GLMs were used to compare the unique contributions of each contrast for each ROI for each period. Mean-centered social anxiety (SPAIC-11) was included in the models to assess the impact of social anxiety.

For the anticipation period, the GLM incorporated Condition (Uncertain Threat Anticipation, Certain Threat Anticipation, and Uncertain Safety Anticipation), Region (BST and Ce), and mean-centered social anxiety (SPAIC-11). Because Certain Safety trials were treated as the unmodeled (implicit) baseline, activation estimates were provided for only 3 of the 4 conditions (e.g., Uncertain Threat vs. Certain Safety anticipation). This choice was motivated by the marked psychological similarity between Certain Safety anticipation and typical inter-trial intervals (ITIs) and served to maximize the overall efficiency (trials-of-interest per unit time) of the paradigm compared to a more conventional design with lengthy ITIs. For the presentation period, Certain Safety presentation activation estimates were able to be modeled by using the anticipation baseline, i.e., Certain Safety presentation vs. Certain Safety anticipation. Thus, for the presentation period, the GLM incorporated Valence (Threat/Safety), Temporal Certainty (Uncertain/Certain), Region (BST/Ce), and mean-centered social anxiety (SPAIC-11). Hypothesis testing used spatially unsmoothed data, and significance was assessed using p=0.05 (two-tailed, uncorrected). Analyses were implemented in SPSS (version 27; IBM), and significant interactions were decomposed using simple effects. Figures were created using R Studio (http://www.rstudio.com).

Under the "double dissociation" hypothesis, we would expect acute Threat Presentation to recruit the Ce, Uncertain Threat Anticipation to recruit the BST, and the same pattern but amplified among adolescents with more severe social anxiety. Under the "integration" hypothesis, we would expect that both regions are recruited to a similar degree by Uncertain Threat Anticipation, Uncertain Threat Presentation, Certain Threat Anticipation, and Certain Threat Presentation, and the same, but exaggerated pattern among more socially anxious adolescents.

Sensitivity analyses confirmed that key results remained similar after controlling for biological sex, mean-centered pubertal status, or mean-centered age (not reported). The only noteworthy observation was that younger participants tended to experience greater anxiety across anticipatory conditions, suggesting indiscriminate anxiety (r=-0.25, p=0.05). Dimensional approaches to psychopathology have a number of advantages over traditional case/control approaches (Cuthbert & Insel, 2010; 2013; Kotov et al., 2017; Latzman et al., 2020). Nevertheless, potential case/control differences were explored. The overall pattern of results was broadly consistent with that yielded by the more rigorous dimensional approach (not reported). Exploratory analyses of potential brain-behavior (in-scanner anxiety ratings) relations were not significant (not reported).

Exploratory Whole-Brain Voxelwise Analyses

A series of whole-brain voxelwise analyses allowed us to explore associations between social anxiety severity and activation of cortical regions implicated in adults and youth with extreme social anxiety. Paralleling ROI analyses, omnibus GLMs were implemented for anticipation and presentation conditions with Certain Safety Anticipation serving as the implicit baseline for contrasts. For the anticipation period, omnibus GLMs

incorporating Condition (Uncertain Threat Anticipation, Certain Threat Anticipation, and Uncertain Safe Anticipation) and mean-centered social anxiety (SPAIC-11) was implemented in MRM (McFarquhar et al., 2016). Significance was assessed using TFCE (Smith & Nichols, 2009) cluster-wise permutation analysis with 10,000 permutations per contrast. Significant interactions were decomposed using appropriately masked pairwise contrasts. A conceptually similar omnibus approach was used to model responses to social stimuli presentations as a function of Valence (Threat/Safety), Temporal Certainty (Uncertain/Certain), and social anxiety (mean-centered SPAIC-11). Analyses were implemented in SPM. Significance was assessed using $p<0.05$, whole-brain-corrected for cluster extent $p<0.001$ based on Gaussian random field theory (Worsley, et al. 1996). Significant interactions were decomposed using appropriately masked pairwise contrasts.

Chapter 3: Results

Behavioral Results

Anxiety Ratings

To confirm the validity of the MSTC paradigm and whether variation in social anxiety symptoms (SPAIC-11) influenced the intensity of anticipatory anxiety elicited by the task, we examined ratings of anxiety experienced during the countdown (Figure 3). Results revealed main effects of Valence ($F[1, 64]=46.71$, $p<0.001$) and Temporal Certainty ($F[1, 64]=18.13$, $p<0.001$), which were tempered by a significant interaction (Social Anxiety × Valence: $F[1, 64]=7.81$; $p=0.01$). As shown in Figure 3, waiting to receive social threat increased anxiety ($t[65]=6.55$; $p<0.001$) and waiting to receive any social stimuli when the timing was uncertain increased anxiety ($t[65]=4.29$, $p<0.001$). These findings are somewhat consistent with prior work using temporally uncertain-threat tasks in adult populations (Somerville et al., 2013; Hur et al., 2020), which show a similar pattern of elevated anxiety but also particularly heightened anxiety for anticipation of uncertain threat outcomes. Our current observations did not demonstrate this effect at a significant level (Valence × Temporal Certainty: $F[1, 64]=1.03$; $p=0.31$). With regard to social anxiety, adolescents with more severe symptoms reported elevated anticipatory anxiety across conditions ($F[1, 64]=4.80$, $p=0.03$; See Figure 4), although this was more evident during the anticipation of social threat ($r=0.33$, $p=0.01$; See Figure 4) compared to mildly positive social stimuli ($r=0.13$, $p=0.31$). Other effects were not significant ($ps > 0.73$). Taken together, these observations confirm the validity of the MSTC task, and provide evidence of both indiscriminate distress and potentiated threat reactivity among socially anxious adolescents.

fMRI Results

EAc ROIs

To evaluate competing hypotheses regarding the role of the EAc in threat processing, we extracted averaged standardized contrast coefficients using anatomically defined, *a priori* Ce and BST ROIs. Standard mixed-effects GLMs were used to compare the unique contributions of each contrast for each ROI for each period. Mean-centered social anxiety (SPAIC-11) was included in the models to assess the impact of social anxiety.

Anticipation. The MSTC paradigm takes the conceptual form of a 2 (Valence) × 2 (Temporal Certainty) design. For maximal efficiency, the anticipation period of Certain Safety trials served as the unmodeled baseline for first-level modeling of the BOLD signal. Thus, hypothesis testing focused on anticipatory activity in the Ce and BST for the three remaining conditions: Uncertain Threat, Certain Threat, and Uncertain Safety, each estimated relative to the implicit baseline (**Figure 5**). A mixed-effects GLM revealed main effects of Region (F [1, 64]=4.86; p=0.03) and Condition (F [2, 128]=3.99; p=0.02), which were tempered by significant Condition × Social Anxiety (F[2, 128]=5.87; p=0.004) and Condition × Region × Social Anxiety interactions (F[2, 128]=4.75; p=0.01).

To decompose this main effect of Region, separate analyses were performed for the Ce and BST. While the Ce proved more responsive than the BST on average (F[1,64]=4.86, p=0.03; see **Figure 6**), this effect was qualified by a significant Condition × Region × Social Anxiety interaction (F[2, 128]=4.75; p=0.01). In the BST, a significant Condition × Social Anxiety interaction was observed (F[2, 128]=6.50, p=0.002); however, anticipatory activity was not significantly related to social anxiety symptoms for any one of the three

conditions (r<.18, p>.15), precluding decisive inferences. The Condition × Social Anxiety interaction was not significant in the Ce (F[2, 128]=1.13, p=0.33).

To decompose the main effect of Condition, relations between the three anticipation conditions (Uncertain Threat, Certain Threat, and Uncertain Safety) were investigated. Uncertain Threat anticipation was associated with greater EAc (Ce/BST) activation than Certain Threat anticipation (t[65]=2.48, p=0.02; **see Figure 6**). At a trend level, Uncertain Threat anticipation was associated with greater EAc activation than Uncertain Safety anticipation (t[65]=1.94, p=0.06). EAc anticipatory activity did not differ between the Certain Threat and Uncertain Safety conditions (t[65]=-0.39, p=0.70). These effects were tempered by a significant Condition × Social Anxiety (F[2, 128]=5.87, p=0.004) interaction, such that adolescents with more severe social anxiety symptoms showed reduced EAc activation during Uncertain-Threat anticipation at a trend level (r= -0.23, p=0.07; **Figure 7**). Remaining relations between social anxiety and condition-specific anticipatory activity were not significant (|r|<0.08, p>0.53; **Figure 8**), and other contrasts were not significant (F<0.55, p>0.46). Overall, these observations demonstrate that the Ce is more sensitive to anticipatory periods when compared to the BST, suggesting the Ce may serve a distinct role in socially salient anticipation processes. However, findings also indicate that the BST and Ce—the two major subdivisions of the EAc—show a similar pattern of recruitment during the uncertain anticipation of social threat and provide marginal evidence that this effect is diminished among adolescents with more severe social anxiety symptoms.

Presentation. In contrast to the anticipation period, separate estimates of activity were available for each of the four presentation conditions. Thus, hypothesis testing

employed a 2 (Valence) × 2 (Temporal Certainty) × 2 (Region) × Social Anxiety (SPAIC-11) mixed effects GLM. Results revealed that threatening faces and voices elicited greater EAc activation (Valence: $F[1, 64]=8.00$; $p=0.01$) and the Ce was more responsive to faces and voices (Region: $F[1, 64]=11.60$; $p=0.001$; **Figure 9**). These findings suggest that while the Ce shows increased recruitment relative to BST in response to presentation of faces and voices, collectively, the BST and Ce together are more sensitive to social threat-related stimuli than safety-related stimuli.

Whole-Brain

A series of whole-brain voxelwise analyses allowed us to explore the role of cortical regions implicated in adults and youth with extreme social anxiety. Paralleling ROI analyses, omnibus GLMs were implemented for anticipation and presentation conditions with Certain Safety Anticipation serving as the implicit baseline for contrasts. At the whole-brain level, there were no significant associations between social anxiety severity (SPAIC-11) and variations in brain response to the MSTC task.

Task effects provided confirmation that the MTSC recruited brain regions implicated in threat anticipation and face and auditory processing. For example, frontocortical regions—including MCC and dlPFC/FP—showed greater activation during the temporally *uncertain* (versus certain) anticipation of social threat, consistent with prior work in typical populations (Hur et al., 2020). Heightened activity during the presentation of social threat (face/voice pairs) relative to safety-related stimuli was evident in systems involved in processing faces (e.g., fusiform gyrus), and voices (e.g., Heschl's gyrus and planum temporale). Additional task effect results are detailed in supplementary tables in the Appendix (see Supplemental Tables 1-20).

Chapter 4: Discussion

Aberrations in threat processing, both when social threat is certain-and-immediately present and when social threat is uncertain-and-remote but anticipated, are hallmarks of social anxiety. Despite the public health burden of extreme forms of social anxiety and the need to develop new treatments, the neural systems recruited during the anticipation and presentation of social threat remain unclear. Further, adolescence is a period of peak vulnerability for more significant and persistent forms of SAD (Haller et al., 2015), but prior work has not yet examined neural substrates of both types of social threat processes during adolescence. Evidence gleaned from two decades of animal research and emerging human neuroimaging work highlights the role of the EAc—which includes the major subdivisions the BST and Ce—in individuals with extreme anxiety and anxiety-related disorders, but specific contributions of these regions to threat processes remains contentious. We sought to address existing gaps by examining the impact of social anxiety severity on EAc function during the anticipation of temporally uncertain social threat and presentation of social threat.

The present results failed to show significant relations between neural systems underpinning social threat processes and social anxiety in adolescence. However, analyses targeting the EAc indicated a trend-level association between heightened anxiety symptoms and hypoactivation of the EAc during temporally uncertain social threat anticipation. These findings do not align with our predictions nor with the preponderance of evidence from existing work in individuals with anxiety disorders showing associations between clinical anxiety and *increased* EAc activation during anticipatory threat processing (e.g., Figel et al., 2019; Buff et al., 2017; Brinkmann et al., 2017a; 2017b) and

presentation of social threat (i.e., faces) in SAD (Brühl et al., 2014; Hattingh et al., 2013). Notably, adolescents with heightened levels of social anxiety reported increased anticipatory anxiety during the task, particularly when anticipating social threat. Consistent with prior work assessing distress during threat anticipation in anxiety disorders (Figel et al., 2019; Buff et al., 2017; Brinkmann et al., 2017a; 2017b), these findings confirm the task was sensitive to individual differences in social anxiety.

Taken together, current observations hint at a potentially unique role of the EAc in adolescent social anxiety. Specifically, the trend-level association between heightened social anxiety symptoms and hypoactivation of the EAc is an unexpected observation and not consistent with existing work. Given that the role of the EAc in temporally uncertain social threat has never before been explored in socially anxious adolescents, these divergent findings could be attributed to the adolescent developmental period and the variability introduced by associated factors such as changing peer dynamics, brain maturation, and pubertal development (e.g., Ferri, Bress, Eaton, & Proudfit, 2014, Kaczkurkin et al., 2016; Vijayakumar, Pfeifer, Flournoy, Hernandez, & Dapretto, 2019). Our current observations might be further clarified by more direct investigation of relevant developmental factors (e.g., ensuring a range of pubertal developmental stages among subject) and comparisons with adult and pre-adolescent populations using cross-sectional or longitudinal designs.

There are potential explanations as to why social anxiety severity in adolescents failed to show significant relations with brain activity. First, the safety baseline, which served as the comparison point for estimates of brain activation elicited by threat and temporal uncertainty, may not have represented a true safety baseline for individuals with

high levels of social anxiety. The current paradigm utilized a social baseline, specifically predictable anticipation of faces with happy expressions and relatively benign statements. A recent study investigating face processing among a large sample of SAD patients (*n*=80) demonstrated increased amygdala activation in response to happy faces relative to angry faces (Crane, Chang, Kinney, & Klumpp, 2021). In addition, both happy faces and neutral faces and criticism and praise have been found to elicit increased activation in the amygdala as well as aberrant frontocortical responses in patients with social anxiety when compared to healthy controls (Birk et al., 2019; Birbaumer et al., 1998; Cooney et al., 2006; Filkowski & Haas, 2017; Gentili et al., 2008; Straube, Mentzel, & Miltner, 2005). Further, emerging research and theoretical models suggest socially anxious individuals fear evaluation in general (Heimberg et al., 2014; Reichenberger et al., 2019; Rodebaugh et al., 2012), and that fear of positive evaluation is a distinct construct relevant in SAD (Fredick & Luebbe, 2020). Thus, in exploring neural correlates of social anxiety, control conditions that utilize social information as a baseline may induce unintended effects in participants, which in turn can weaken the ability of a paradigm to capture clinically meaningful comparisons.

The social threat presentation in our paradigm, static faces with angry expressions and audio recordings of negative evaluative statements, perhaps did not elicit robust fear of negative evaluation, a defining feature of SAD. Although social threat presentation elicited increased momentary anxiety during anticipation periods, examination of mean data suggests these momentary increases were modest in size. Further, momentary anxiety does not cleanly map onto the concept of fear of negative evaluation, a more complex construct with meaningful social context. Due to the artificial nature of our task, increases in momentary anxiety during our paradigm likely related to anticipation of an aversive

stimuli presentation, rather than anticipation of actual evaluation. That is, participants are likely experiencing anxiety and distress related to incoming *aversive* stimuli, rather than incoming *negative evaluation.* Patterns of brain activation typically observed in individuals with SAD when viewing negative emotional faces, such as aberrant activity in fronto-amygdala circuits, are not unique to the disorder. These patterns also occur in individuals with generalized anxiety disorder (Monk et al., 2006; 2008; Thomas et al., 2001) and other psychiatric conditions including major depressive disorder (Beesdo et al., 2009), post-traumatic stress (Garett et al., 2012), and ADHD (Brotman et al., 2010), potentially reflecting shared disruptions to emotional face processing across psychopathology. The current study included adolescents who met criteria for other internalizing disorders and ADHD but who did not exhibit high levels of social anxiety symptoms, nor low levels of social anxiety symptoms (i.e., extreme SPAIC-11 scores). As a result, the possibility of finding social-anxiety-specific differences among brain regions recruited during a task that was sensitive to multiple forms of psychopathology was reduced.

Defining and modeling SAD-specific processes in neuroimaging studies remains a key challenge for future work and limits the ability to apply existing accounts of EAc function in threat anticipation processes to *social* threat anticipation processes. Existing work targeting anticipatory responding in social anxiety has successfully probed the EAc by implementing more ecologically-valid forms of social evaluation with a nonsocial baseline, such as video camera observation versus absence of video camera observation (Figel et al., 2019). Future work should utilize similar strategies, specifically more naturalistic paradigms inducing more explicit evaluation threat and a nonsocial baseline, to clarify identified findings from the present study as well as extend models of threat

processing and EAc function in adolescent social anxiety. Paradigms can be further enriched by collecting in-scanner ratings using an expanded scale (to mitigate floor and ceiling effects) on every trial (instead of 4 times per run as in the current MSTC task), which would enable within-subject mediation analysis (Pessoa & Padmala, 2005). Additionally, leveraging resting or dynamic arterial spin labeling (ASL), an MRI technique for measuring tissue perfusion (i.e., blood flow), in future studies of social threat processes could advance current understanding of EAc function. Because ASL provides a meaningful baseline calibrated to real physical units, the technique allows assessment of group differences in each condition, not just relative differences (e.g., a condition versus an implicit baseline as in fMRI). Thus, future work using ASL could assess whether social anxiety in adolescence indiscriminately elevates EAc activity (e.g., Kaczkurkin et al., 2016).

While relations between social anxiety and the MSTC remain inconclusive, task effects among all participants yielded several key findings. Consistent with prior work in youth and adults (Brühl et al., 2014; Jarcho et al., 2013), presentation of threat-related social stimuli relative to benign social stimuli demonstrated heightened EAc activation. The EAc also showed sensitivity to temporal uncertainty during anticipation periods. Specifically, temporally uncertain anticipation of social threat compared to certain anticipation of social threat demonstrated increased activation in the Ce and BST. Interestingly, a different pattern was observed in prior work from our group focusing on healthy adults and generalized threat processing, wherein EAc activation was greater for temporally certain anticipation of threat relative to temporally uncertain anticipation of threat (Hur et al., 2020). Direct comparisons of the BST and Ce did not show a condition

by region *or* a condition by valence interaction. Rather, the BST and Ce showed a similar pattern of heightened recruitment during the uncertain anticipation of social threat *and* together were more sensitive social threat-related stimuli than safety-related stimuli. Collectively, our findings provide support for the "integration" account in social threat anticipation and presentation processes. Additionally, results underscore the relevance of temporal uncertainty to enhancing recruitment of the EAc broadly.

Within the context of prior work, these observations contribute to a variable account of EAc response to social threat anticipation and presentation, suggesting replication studies are needed. Figel et al. (2019) found the major subdivisions of the EAc showing similar responses to certain-and-immediate threat for patients with SAD, whereas during temporally uncertain anticipation of social threat, only the BST showed heightened activation for all participants. Importantly, Figel et al. (2019) did not directly compare the major subdivisions of the EAc in the same statistical analysis, precluding the ability to draw strong inferences about relative contributions of the EAc. In Clauss et al. (2019), the BST showed greater recruitment relative to Ce in response to brief cues signaling uncertain social threat anticipation (i.e., unknown valence of face, fearful face occurring at p=0.50). Elevated levels of social anxiety were found to be associated with greater BST than Ce response to unpredictably signaled presentation of threat-related (fearful) faces compared to neutral faces. While task differences limit direct comparison, this pattern of results was not observed in our work, suggesting the EAc may respond differently to temporally uncertain social threat versus uncertain outcomes in which social threat is a possibility.

In general, research targeting EAc function and threat processes shows substantial heterogeneity in study characteristics including the type of unpredictability induced (e.g.,

unpredictable content of anticipated stimuli, temporal unpredictability), content of the anticipated threat stimuli (pictures, electric shocks), which control conditions are included (e.g., unpredictable threat versus predictable threat), and when in the threat processing time course EAc function is estimated (i.e., initial onset of threat anticipation cue, sustained anticipation period, presentation of threat stimuli). For example, some studies assess neural correlates over anticipatory periods spanning several seconds (Tillfors et al., 2002; Lorberbaum et al., 2004; Boehme et al., 2014;), some only assess anticipation at the early information processing stage occurring at the start of an anticipatory cue (1-2 seconds; Clauss et al., 2019, Williams et al., 2015), and others estimate both brief, onset cues initiating the anticipation trial and the sustained anticipation trial (Figel et al., 2019; Davies et al., 2017). These variations in study design, compounded by nomenclature differences across studies, make mapping results onto overarching models of EAc function extremely challenging and hampers progress. A future challenge for the field will be to systematically define and then characterize how specific facets, like type of uncertainty and duration of anticipation, individually and then combined impact EAc activity.

While our sample size is comparable to some recent neuroimaging studies utilizing a dimensional approach in extreme anxiety (e.g., Clauss et al., 2019; Somerville et al., 2013), we were limited in the potential ability to detect individual differences due to our small sample size and complex interactions within hypothesis testing. A key challenge for future research will be to explore EAc function and temporally uncertain social threat anticipation in larger samples to replicate and potentially clarify present findings. Given evidence of sex- and age-based differences in social threat processing (Gold et al., 2020; Im et al., 2018; McClure et al., 2004) and in the EAc (Lebow & Chen, 2016; Wright,

Hostinar, & Trainor, 2020), it will be critical for future work to obtain adequate power to explore potential sex and developmental effects in social threat anticipation and social anxiety. Moreover, improvements to study design will allow researchers to understand how SAD and EAc functioning unfolds throughout development. To capture changes in social threat processing that are embedded with bio-social-emotional developmental factors and their relation to social anxiety severity, it will be necessary to utilize cross-sectional and longitudinal studies (Zacharek, Kribakaran, Kitt, & Gee, 2021). Future work should could include examinations between adolescence and preadolescence and/or adulthood populations as well as different periods within adolescence, such as focusing on comparisons between early, middle, and late adolescence.

Conclusion

Understanding the neural systems governing individual differences in adolescent social anxiety severity is important. Extreme forms of social anxiety in adolescence confer risk for a range of deleterious outcomes spanning academic and socioemotional functioning, health, and well-being. Uncertain-and-remote anticipation of social threat is a core symptom-eliciting feature of social anxiety, yet the neurobiological processes underpinning this feature are unclear. Prominent models of uncertain threat anticipation contend that the central extended amygdala (EAc)—including BST and the Ce—plays a key role in threat processing and anxiety disorders. The present findings failed to find significant associations between social anxiety severity and neural correlates of social threat anticipation and presentation. Trend-level observations hint at the possibility of perturbations in the EAc in response to uncertain social threat anticipation in adolescents with more severe social anxiety. Task effects among all participants extend current models

of EAc function in social threat anticipation and suggest similar patterns of recruitment among the BST and Ce. Our observations inform recommendations for future studies–namely, utilizing a dimensional approach with a larger sample size, incorporating a nonsocial baseline, and probing uncertain-and-remote threat anticipation with more ecologically-valid tasks that induce evaluation.

Tables

Table 1				
Analysis of sex and racial demographic differences in SPAIC-11 scores				
	N	**SPAIC-11 M ± SD**	**t-value**	**p-value**
Male	26	9.47 ± 5.41	0.59	0.56
Female	40	10.37 ± 6.34		
White	33	9.52 ± 6.47	0.67	0.51
Black, Asian, Hispanic/Latinx, Bi/Multiracial, Pacific Islander	33	10.50 ± 5.47		

Figures

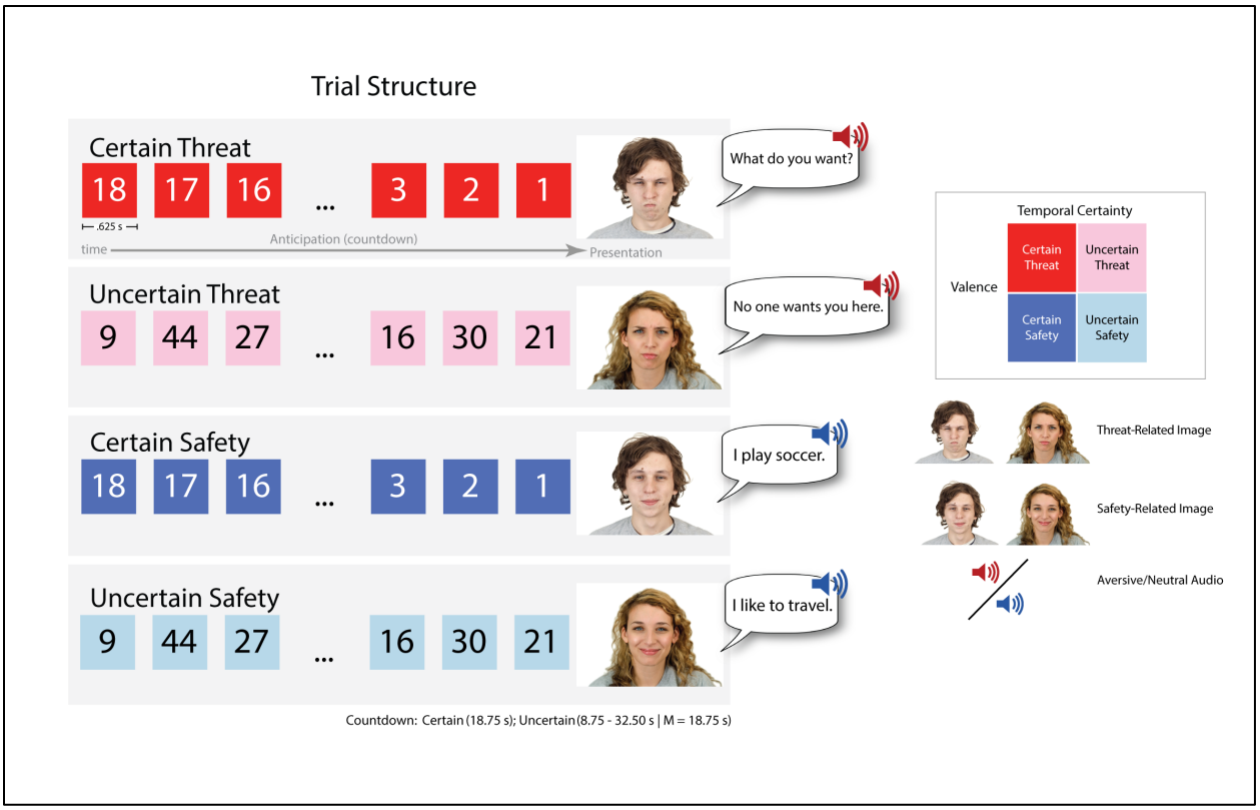

Figure 1. The Maryland Social Threat Countdown (MSTC) paradigm. The MSTC paradigm takes the form of a 2 (*Valence:* Threat/Safety) × 2 (*Temporal Certainty:* Uncertain/Certain) × 2 (*Period:* Anticipation/Presentation) randomized event-related design (3 scans; 6 trials per condition; 4 conditions per scan). On Certain Threat trials, participants saw a descending stream of integers ("count-down"; e.g., 30, 29, 28...3, 2, 1) for 18.75 seconds. This anticipation period always culminated with the presentation period, the delivery of a socially threatening photograph (angry face) and audio clip (e.g., *"No one wants you here"*). Uncertain Threat trials were similar, but the integer stream was randomized and presented for an uncertain and variable duration (8.75-32.50 seconds; *M*=18.75 seconds). Here, subjects knew that social threat was going to be delivered, but they had no way of knowing precisely *when* it would occur. Safety trials were similar but terminated with the delivery of comparatively benign photographs (happy face) and audio clips (*"I play soccer."*). Valence was continuously signaled during the anticipation period by the background color of the display. Participants provided ratings of anticipatory fear/anxiety for each trial type during each scan. Simulations were used to ensure the separability of task-related hemodynamic signals (variance inflation factors < 1.68).

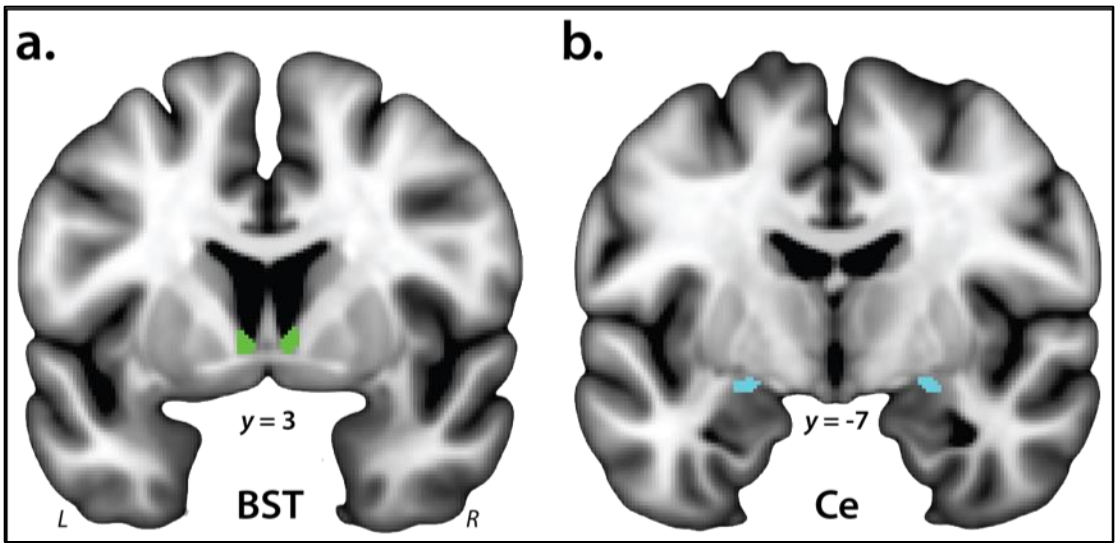

Figure 2. BST and Ce ROIs. **a.** BST. The derivation of the probabilistic BST ROI (green) is detailed in Theiss, Ridgewell, McHugo, Heckers, and Blackford (2017) and was thresholded at 25%. The seed mostly encompasses the supra-commissural BST, given the difficulty of reliably discriminating the borders of regions below the anterior commissure on the basis of T1-weighted images (Kruger, Shiozawa, Kreifelts, & Ethofer, 2015). **b.** Ce. The derivation of the Ce ROI (cyan) is described in more detail in Tillman et al. (2018). For illustrative purposes, 1-mm ROIs are shown. Analyses employed ROIs decimated to the 2-mm resolution of the EPI data. Abbreviations—BST, bed nucleus of the stria terminalis; Ce, central nucleus of the amygdala; L, left hemisphere; R, right hemisphere.

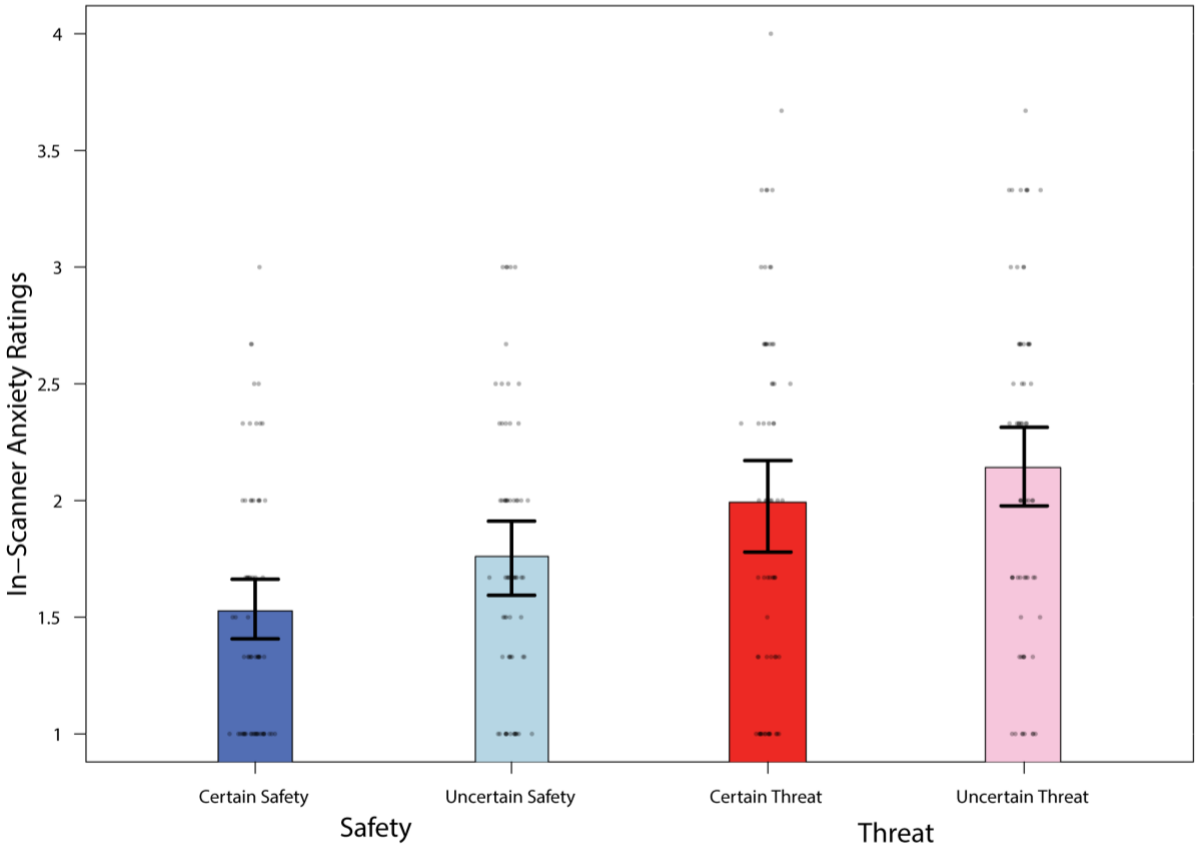

Figure 3. Ratings of in-scanner momentary anxiety (black points; individual participants), Bayesian 95% highest density interval (black bars), and mean (colored bins) for each condition. Highest density intervals permit population-generalizable visual inferences about mean differences and were estimated using 1000 samples from a posterior Gaussian distribution.

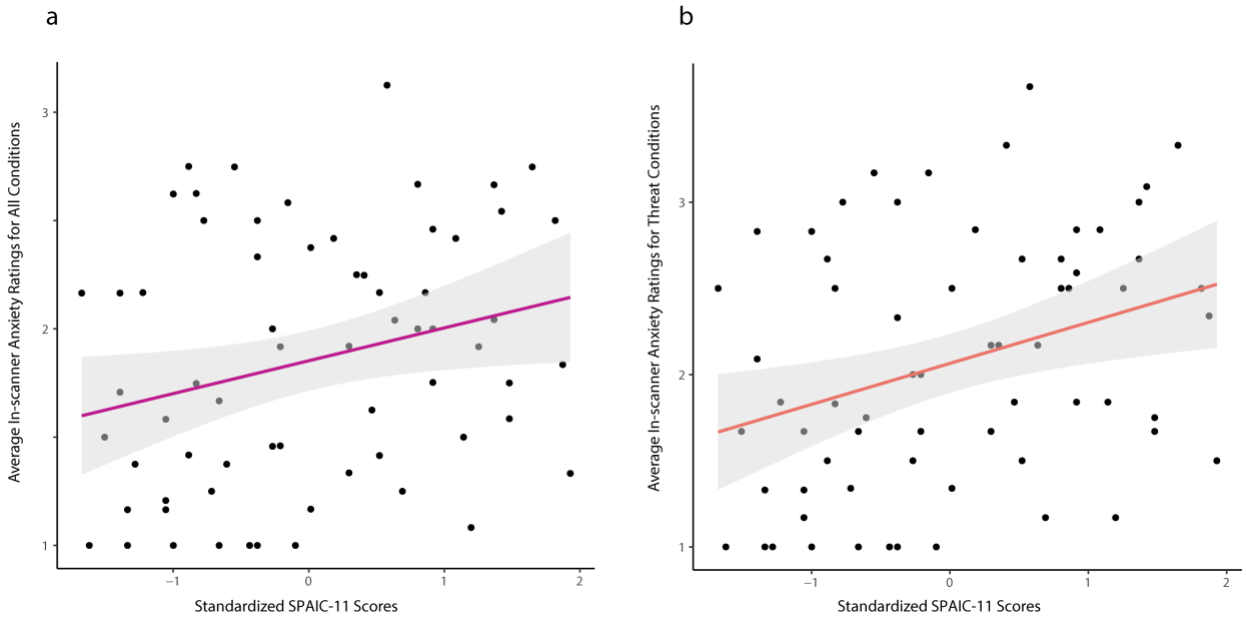

Figure 4. **a.** Relations between ratings of anxiety elicited from all conditions in the Maryland Social Threat Countdown paradigm and self-reported social anxiety symptom severity (standardized scores from the Social Phobia and Anxiety Inventory for Children abbreviated questionnaire [SPAIC-11]). **b.** Relations between ratings of distress elicited from Threat conditions (collapsed across temporal uncertainty and certainty) in the Maryland Social Threat Countdown paradigm and self-reported social anxiety symptom severity (standardized scores from the Social Phobia and Anxiety Inventory for Children abbreviated questionnaire [SPAIC-11])

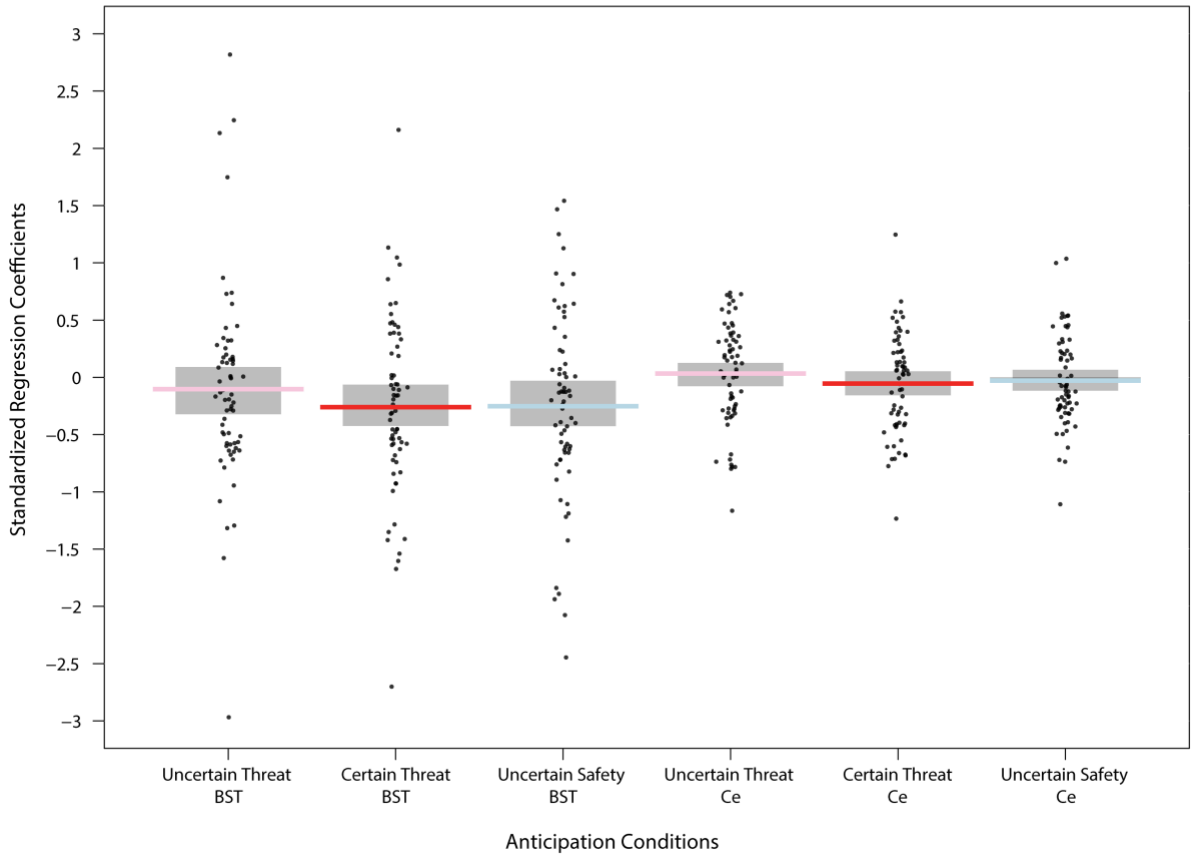

Figure 5. Data (black points; individual participants), Bayesian 95% highest density interval (gray bands), and mean (bars) for each condition for each region of interest. Highest density intervals permit population-generalizable visual inferences about mean differences and were estimated using 1000 samples from a posterior Gaussian distribution.

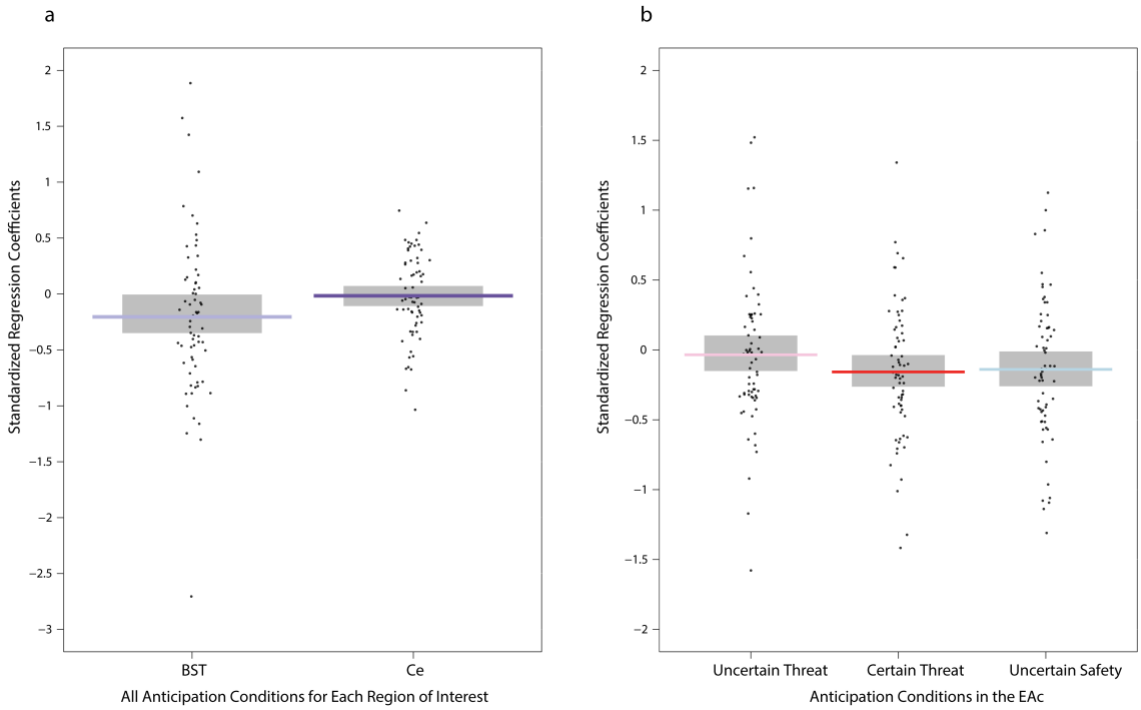

Figure 6. **a.** Data (black points; individual participants), Bayesian 95% highest density interval (gray bands), and mean (bars) for each region of interest (BST/Ce) collapsed across all conditions (Uncertain Threat Anticipation/Certain Threat Anticipation/ Uncertain Safety Anticipation). **b.** Data (black points; individual participants), Bayesian 95% highest density interval (gray bands), and mean (bars) for each condition (Uncertain Threat Anticipation/Certain Threat Anticipation/ Uncertain Safety Anticipation) in the EAc (BST/Ce). Highest density intervals permit population-generalizable visual inferences about mean differences and were estimated using 1000 samples from a posterior Gaussian distribution.

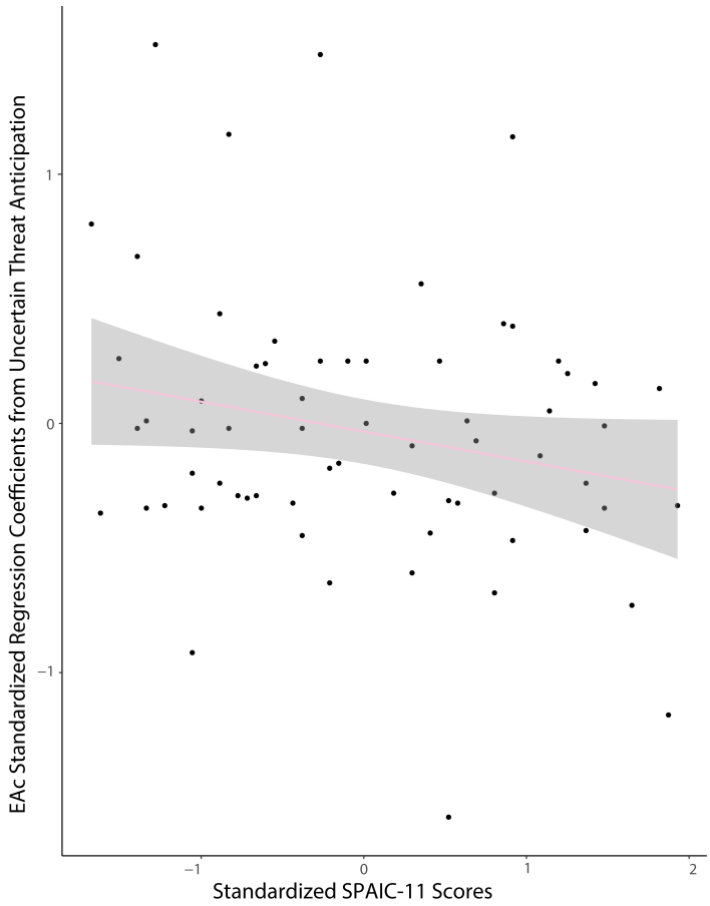

Figure 7. Relationship between Uncertain Threat anticipatory activation in the BST and Ce, subdivisions of the central extended amygdala (activation from regions of interest collapsed), and self-reported social anxiety symptom severity (standardized scores from the Social Phobia and Anxiety Inventory for Children questionnaire [SPAIC-11]).

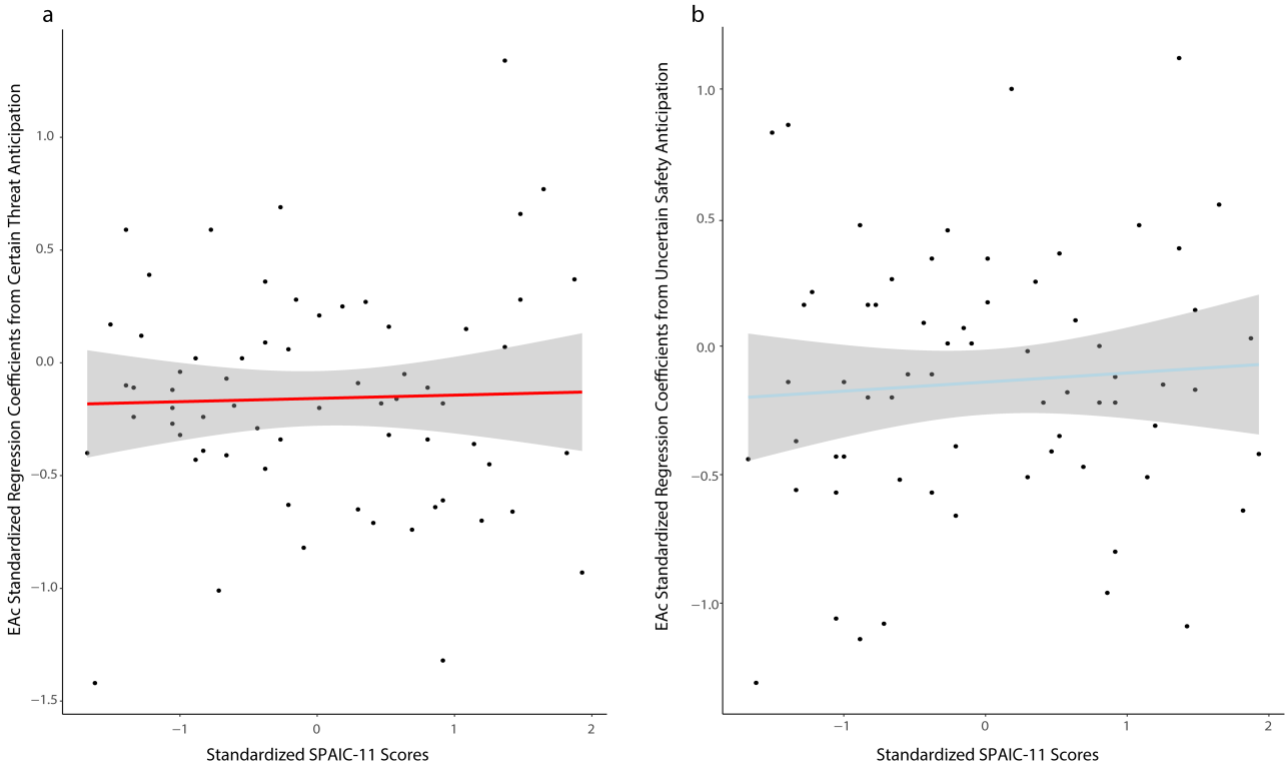

Figure 8. Relationships between other anticipatory conditions in the BST and Ce, subdivisions of the central extended amygdala (activation from regions of interest collapsed), and self-reported social anxiety symptom severity (standardized scores from the Social Phobia and Anxiety Inventory for Children questionnaire [SPAIC-11]) **a.** Certain Threat anticipatory activation in the central extended amygdala and self-reported social anxiety symptom severity (r= -0.02, p=0.88); **b.** Uncertain Safety anticipatory activation in the central extended amygdala and self-reported social anxiety symptom severity (r=0.08, p=0.53).

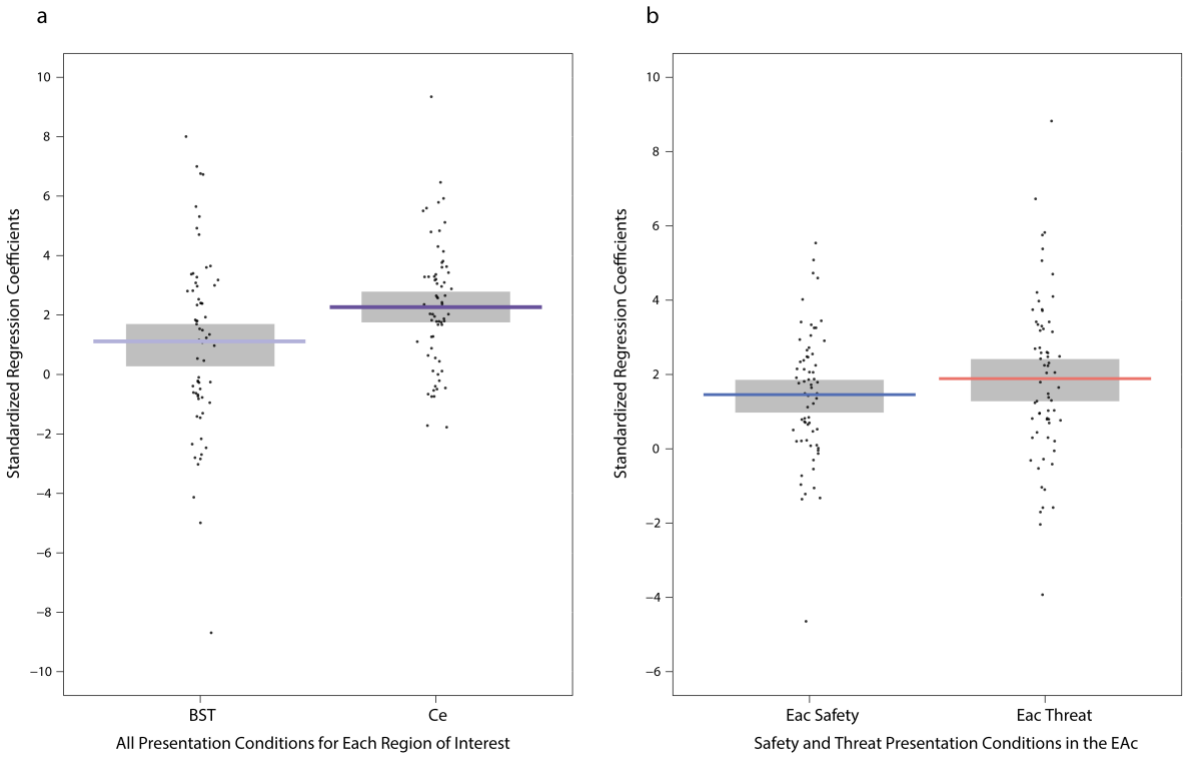

Figure 9. **a.** Data (black points; individual participants), Bayesian 95% highest density interval (gray bands), and mean (bars) for each region of interest (BST/Ce) collapsed across all conditions (Uncertain Threat Presentation/Certain Threat Presentation/ Uncertain Safety Presentation/ Certain Safety Presentation). **b.** Data (black points; individual participants), Bayesian 95% highest density interval (gray bands), and mean (bars) for Threat and Safety conditions (mean of Uncertain Threat Presentation and Certain Threat Presentation/ mean of Uncertain Safety Presentation and Certain Safety Presentation) in the EAc (BST/Ce). Highest density intervals permit population-generalizable visual inferences about mean differences and were estimated using 1000 samples from a posterior Gaussian distribution.

Appendices

Appendix A: Social Anxiety Severity measure (SPAIC-11) and Anxiety Interference Questions from Preliminary Screening

Social Anxiety Severity Measure – The Social Phobia and Anxiety Inventory for Children-11

Think about yourself and choose the option that describes how often you would feel nervous or scared when doing this.

	Never or Hardly Ever	Sometimes	Most of the time or Always
I feel scared when I am with other boys and girls or adults and I have to do something while they watch me (read aloud, play a game, play a sport).	○	○	○

Think about yourself and choose the option that describes how often you would feel nervous or scared when doing this.

	Never or Hardly Ever	Sometimes	Most of the time or Always
I feel scared when I have to speak or read in front of a group of people.	○	○	○

Think about yourself and choose the option that describes how often you would feel nervous or scared when doing this.

	Never or Hardly Ever	Sometimes	Most of the time or Always
I usually do not speak to anyone until they speak to me.	○	○	○

If somebody starts arguing with me, I feel scared and do not know what to do if that person is:

	Never or Hardly Ever	Sometimes	Most of the time or Always
A boy or girl my age that I know	○	○	○
A boy or girl my age that I don't know	○	○	○
An Adult	○	○	○

If somebody asks me to do something that I don't want to do, I feel scared and don't know what to say if that person is:

	Never or Hardly Ever	Sometimes	Most of the time or Always
A boy or girl my age that I know	○	○	○
A boy or girl my age that I don't know	○	○	○
An Adult	○	○	○

I feel scared and don't know what to do when in an embarrassing situation with:

	Never or Hardly Ever	Sometimes	Most of the time or Always
A boy or girl my age that I know	○	○	○
A boy or girl my age that I don't know	○	○	○
An Adult	○	○	○

If somebody says something that I think is wrong or bad, I feel scared saying what I think if that person is:

	Never or Hardly Ever	Sometimes	Most of the time or Always
A boy or girl my age that I know	○	○	○
A boy or girl my age that I don't know	○	○	○
An Adult	○	○	○

I feel scared when I start to talk to:

	Never or Hardly Ever	Sometimes	Most of the time or Always
A boy or girl my age that I know	○	○	○
A boy or girl my age that I don't know	○	○	○
An Adult	○	○	○

I feel scared if I have to talk for longer than a few minutes with:

	Never or Hardly Ever	Sometimes	Most of the time or Always
A boy or girl my age that I know	○	○	○
A boy or girl my age that I don't know	○	○	○
An Adult	○	○	○

I feel scared when speaking (giving a book report, reading in front of the class) in front of:

	Never or Hardly Ever	Sometimes	Most of the time or Always
A boy or girl my age that I know	○	○	○
A boy or girl my age that I don't know	○	○	○
An Adult	○	○	○

I feel scared when I am in a school play, choir, music or dance recital in front of:

	Never or Hardly Ever	Sometimes	Most of the time or Always
A boy or girl my age that I know	○	○	○
A boy or girl my age that I don't know	○	○	○
An Adult	○	○	○

Anxiety Interference Questions from Preliminary Screening

How much of an effect does anxiety have on your life? For example, do you ever pretend to be sick to get out of a presentation or group project, avoid social activities, etc.?

- ○ Not at all
- ○ Slightly
- ○ Moderately
- ○ Very
- ○ Extremely

How much does anxiety "mess things up" for you? For example, does it ever cause you to not participate in class, cause problems in your friendships, etc.?

- Not at all
- Slightly
- Moderately
- Very
- Extremely

How much does anxiety bother you or cause you distress? For example, does it ever make you feel alone or bad about yourself, cause you to worry about what others are thinking a lot of the time, etc.?

- Not at all
- Slightly
- Moderately
- Very
- Extremely

Appendix B: Diagnostic Breakdown of Participant Sample

	High social anxiety (*N=24)*	Intermediate social anxiety (*N=18)*	Low social anxiety (*N=30)*
Major Depressive Disorder	8	1	0
Dysthymia	3	1	0
Panic Disorder	5	2	0
Separation Anxiety Disorder	1	0	0
Social Anxiety Disorder	24	0	0
Specific Phobia	4	0	0
Post-traumatic stress disorder	3	0	0
Attention-deficit/hyperactivity disorder	2	2	0
Generalized Anxiety Disorder	12	1	0

Appendix C: Verbatim Instructions from the Practice Version of the Maryland Social Threat Countdown Paradigm

"Welcome to the Practice Face Task! (press any button to continue)";
"In this task, you will see faces and hear pleasant or unpleasant statements. They might look like this: (press any button to continue) ";

*** threat-related face with aversive statement is presented***
safety-related face with neutral statement is presented
"Sometimes, you will know when the faces and statements are coming. Numbers will countdown to the picture. Sometimes, you will not know when the faces and statements are coming. The numbers will be random and not tell you when the picture is coming (press any button for examples)";
Certain countdown culminating with threat-related face and aversive statement is presented
Uncertain countdown culminating with safety-related face and neutral statement is presented
“You will be able to tell whether the face and statement will be pleasant or unpleasant based on the color of the background during the countdown. Red lets you know it will be unpleasant, and blue lets you know it will be pleasant”
"Every once in a while, we will ask you to rate how anxious you were before the last picture. (press any button for an example)"
***Ratings Prompt presented which reads: “Please rate your anxiety during the last condition [1/least anxious – 4/most anxious]” ***
" Great job! Any questions? "

Appendix D: Supplemental Tables

Supplemental Table 1. Descriptive statistics for clusters and local extrema showing differences in activation between the three Anticipation conditions (Uncertain Threat/Certain Threat Anticipation/Uncertain Safe Anticipation; whole-brain corrected with cluster-wise permutation analysis with 10,000 permutations per contrast).

Cluster	Left / Right	Label	mm^3	*F*	x	y	z
1	L	Cuneal Cortex	86,824	8.96	-12	-80	30
1	L	Intracalcarine Cortex	86,824	89.58	-14	-74	8
1	L	Lateral Occipital Cortex, superior division	86,824	10.68	-12	-84	46
1	L	Lingual Gyrus	86,824	17.71	-18	-52	-10
1	L	Occipital Fusiform Gyrus	86,824	32.06	-28	-72	-12
1	L	Occipital Pole	86,824	61.57	-8	-98	-4
1	L	Temporal Occipital Fusiform Cortex	86,824	23.56	-32	-58	-14
1	R	Cuneal Cortex	86,824	26.25	4	-86	34
1	R	Intracalcarine Cortex	86,824	130.35	14	-78	12
1	R	Lingual Gyrus	86,824	17.54	18	-44	-10
1	R	Occipital Fusiform Gyrus	86,824	43.76	26	-76	-12
1	R	Occipital Pole	86,824	69.28	8	-90	-2
1	R	Supracalcarine Cortex	86,824	104.29	2	-80	8
1	R	Temporal Occipital Fusiform Cortex	86,824	14.71	28	-48	-12
2	L	Postcentral Gyrus	48,576	8.68	-14	-46	70
2	L	Precuneus Cortex	48,576	16.41	-10	-50	58
2	L	Superior Parietal Lobule	48,576	17.66	-28	-46	60
2	R	Angular Gyrus	48,576	17.94	60	-46	22
2	R	Lateral Occipital Cortex, inferior division	48,576	46.47	48	-72	0
2	R	Lateral Occipital Cortex, superior division	48,576	23.03	48	-68	20
2	R	Middle Temporal Gyrus, temporooccipital part	48,576	23.57	60	-46	2
2	R	Postcentral Gyrus	48,576	14.62	42	-36	58
2	R	Precuneus Cortex	48,576	16.16	8	-48	54
2	R	Superior Parietal Lobule	48,576	18.55	26	-50	52
2	R	Supramarginal Gyrus, posterior division	48,576	17.66	44	-38	50
2	R	Temporal Occipital Fusiform Cortex	48,576	27.99	44	-50	-16
3	R	Middle Frontal Gyrus	8,360	11.27	28	12	54
3	R	Precentral Gyrus	8,360	18.63	26	-12	66
3	R	Superior Frontal Gyrus	8,360	15.01	20	-2	58
4	L	Middle Frontal Gyrus	8,080	11.80	-38	4	46
4	L	Paracingulate Gyrus	8,080	14.49	-10	12	44

4	L	Precentral Gyrus	8,080	16.97	-32	-10	56
4	L	Superior Frontal Gyrus	8,080	15.40	-12	6	64
4	R	Midcingulate Cortex	8,080	17.13	6	8	26
4	R	Paracingulate Gyrus	8,080	9.35	6	14	40
5	R	Inferior Frontal Gyrus, pars opercularis	7,576	21.36	40	12	26
5	R	Precentral Gyrus	7,576	30.19	46	8	32
6	R	Frontal Pole/ dorsolateral Prefronal Cortex	3,216	14.79	26	42	28
6	R	Middle Frontal Gyrus	3,216	12.03	32	34	32
7	L	Inferior Temporal Gyrus, temporooccipital part	2,800	15.91	-46	-62	-12
7	L	Middle Temporal Gyrus, posterior division	2,800	10.41	-58	-44	-2
7	L	Middle Temporal Gyrus, temporooccipital part	2,800	12.94	-56	-50	2
8	L	Midcingulate Cortex	1,096	11.69	-10	24	26
9	L	Lateral Occipital Cortex, superior division	1,096	13.78	-22	-76	36

Supplemental Table 2. Descriptive statistics for clusters and local extrema showing greater activity during the Anticipation of Uncertain Threat relative to Certain Threat (pairwise contrasts masked by omnibus test between anticipation conditions [F-test]).

Cluster	**Left / Right**	**Label**	**mm³**	***t***	**x**	**y**	**z**
1	R	Angular Gyrus	38,152	5.57	62	-46	18
1	R	Lateral Occipital Cortex, inferior division	38,152	8.48	52	-72	-2
1	R	Lateral Occipital Cortex, superior division	38,152	4.95	22	-68	42
1	R	Middle Temporal Gyrus, temporooccipital part	38,152	6.95	60	-46	2
1	R	Postcentral Gyrus	38,152	4.87	42	-36	58
1	R	Superior Parietal Lobule	38,152	5.17	24	-50	54
1	R	Supramarginal Gyrus, posterior division	38,152	5.78	42	-40	48
1	R	Temporal Occipital Fusiform Cortex	38,152	6.74	44	-50	-18
2	L	Postcentral Gyrus	8,064	4.22	-14	-46	70
2	L	Precuneus Cortex	8,064	5.65	-10	-50	56
2	L	Superior Parietal Lobule	8,064	6.00	-28	-46	60
2	R	Lateral Occipital Cortex, superior division	8,064	4.47	14	-62	54
2	R	Precuneus Cortex	8,064	5.72	10	-46	52
3	R	Middle Frontal Gyrus	7,624	4.78	28	12	54
3	R	Precentral Gyrus	7,624	5.11	38	-6	50
3	R	Superior Frontal Gyrus	7,624	5.14	22	4	52
4	R	Inferior Frontal Gyrus, pars opercularis	7,576	6.33	40	12	26
4	R	Precentral Gyrus	7,576	7.63	44	6	32
5	L	Middle Frontal Gyrus	7,432	4.76	-40	4	46
5	L	Paracingulate Gyrus	7,432	5.46	-10	12	44
5	L	Precentral Gyrus	7,432	5.38	-32	-8	56

5	L	Superior Frontal Gyrus	7,432	4.81	-26	0	62
5	R	Midcingulate Cortex	7,432	4.89	8	24	28
5	R	Paracingulate Gyrus	7,432	4.08	2	12	42
6	R	Frontal Pole	3,184	5.29	26	42	28
7	L	Inferior Temporal Gyrus, temporooccipital part	2,648	5.49	-46	-62	-12
7	L	Middle Temporal Gyrus, posterior division	2,648	4.32	-58	-44	-2
7	L	Middle Temporal Gyrus, temporooccipital part	2,648	4.87	-56	-50	4
8	L	Midcingulate Cortex	1,080	4.79	-10	24	26
9	L	Lateral Occipital Cortex, superior division	1,072	5.29	-24	-76	36
10	R	Midcingulate Cortex	384	5.29	4	12	24
11	L	Cuneal Cortex	40	3.68	-12	-82	30

Supplemental Table 3. Descriptive statistics for clusters and local extrema showing greater activity during the Anticipation of Certain Threat relative to Uncertain Threat (pairwise contrasts masked by omnibus test between anticipation conditions [F-test]).

Cluster	**Left / Right**	**Label**	**mm³**	***t***	**x**	**y**	**z**
1	L	Intracalcarine Cortex	82,288	11.82	-14	-74	6
1	L	Lateral Occipital Cortex, inferior division	82,288	4.06	-38	-86	-16
1	L	Lingual Gyrus	82,288	5.57	-18	-52	-10
1	L	Occipital Fusiform Gyrus	82,288	7.64	-28	-76	-12
1	L	Occipital Pole	82,288	11.13	-8	-98	-4
1	L	Temporal Occipital Fusiform Cortex	82,288	6.57	-32	-58	-14
1	R	Cuneal Cortex	82,288	7.03	2	-86	36
1	R	Intracalcarine Cortex	82,288	11.50	12	-88	2
1	R	Occipital Fusiform Gyrus	82,288	9.19	26	-76	-12
1	R	Occipital Pole	82,288	11.94	6	-90	-2
1	R	Supracalcarine Cortex	82,288	12.56	2	-80	8
2	R	Lingual Gyrus	504	4.98	18	-44	-10
2	R	Temporal Occipital Fusiform Cortex	504	3.33	26	-48	-14

Supplemental Table 4. Descriptive statistics for clusters and local extrema showing greater activity during the Anticipation of Uncertain Threat relative to Uncertain Safety (pairwise contrasts masked by omnibus test between anticipation conditions [F-test]).

Cluster	**Left / Right**	**Label**	**mm³**	***t***	**x**	**y**	**z**
1	L	Precuneus Cortex	3,640	5.16	-6	-50	54
1	R	Cingulate Gyrus, posterior division	3,640	3.82	10	-32	40
1	R	Precuneus Cortex	3,640	4.91	6	-46	54
2	R	Angular Gyrus	880	5.03	60	-46	22
3	L	Lateral Occipital Cortex, superior division	544	4.06	-26	-80	34

4	L	Lateral Occipital Cortex, superior division	16	3.48	-18	-88	36

Supplemental Table 5. Descriptive statistics for clusters and local extrema showing greater activity during the Anticipation of Uncertain Safety relative to Uncertain Threat (pairwise contrasts masked by omnibus test between anticipation conditions [F-test]).

Cluster	Left / Right	Label	mm^3	*t*	x	y	z
1	L	Intracalcarine Cortex	57,272	12.50	-12	-74	10
1	L	Occipital Pole	57,272	7.38	-2	-94	-4
1	R	Cuneal Cortex	57,272	5.92	2	-84	36
1	R	Intracalcarine Cortex	57,272	16.37	14	-78	12
1	R	Occipital Pole	57,272	6.87	14	-102	-2
2	R	Occipital Fusiform Gyrus	992	5.28	30	-68	-12
2	R	Temporal Occipital Fusiform Cortex	992	4.14	34	-60	-12
3	L	Lingual Gyrus	368	5.55	-16	-52	-12
4	R	Lateral Occipital Cortex, inferior division	8	3.37	40	-86	-10

Supplemental Table 6. Descriptive statistics for clusters and local extrema showing greater activity during the Anticipation of Certain Threat relative to Uncertain Safety (pairwise contrasts masked by omnibus test between anticipation conditions [F-test]).

Cluster	Left / Right	Label	mm^3	*t*	x	y	z
1	L	Lingual Gyrus	29,288	7.55	-6	-90	-10
1	L	Occipital Fusiform Gyrus	29,288	6.90	-28	-70	-12
1	L	Occipital Pole	29,288	5.25	-8	-98	2
1	L	Temporal Occipital Fusiform Cortex	29,288	6.26	-32	-56	-14
1	R	Cuneal Cortex	29,288	3.31	6	-86	38
1	R	Lingual Gyrus	29,288	7.98	6	-90	-6
1	R	Occipital Fusiform Gyrus	29,288	8.24	24	-76	-10
1	R	Occipital Pole	29,288	6.75	14	-98	2
1	R	Temporal Occipital Fusiform Cortex	29,288	5.49	28	-48	-12
2	L	Lateral Occipital Cortex, superior division	1,192	3.61	-12	-84	46
2	L	Occipital Pole	1,192	4.94	-14	-90	34
3	L	Precuneus Cortex	56	4.08	-4	-82	42

Supplemental Table 7. Descriptive statistics for clusters and local extrema showing greater activity during the Anticipation of Uncertain Safety relative to Certain Threat (pairwise contrasts masked by omnibus test between anticipation conditions [F-test]).

Cluster	Left / Right	Label	mm^3	*t*	x	y	z
1	R	Inferior Temporal Gyrus, temporooccipital part	21,888	4.84	56	-52	-12
1	R	Lateral Occipital Cortex, inferior division	21,888	9.05	46	-74	0

1	R	Middle Temporal Gyrus, temporooccipital part	21,888	5.74	54	-56	0
1	R	Temporal Occipital Fusiform Cortex	21,888	6.02	46	-56	-18
2	R	Lateral Occipital Cortex, superior division	5,040	4.00	38	-66	34
2	R	Postcentral Gyrus	5,040	4.11	14	-44	62
2	R	Superior Parietal Lobule	5,040	5.14	32	-40	64
2	R	Supramarginal Gyrus, posterior division	5,040	4.27	42	-40	50
3	R	Inferior Frontal Gyrus, pars opercularis	4,136	3.35	54	12	16
4	R	Intracalcarine Cortex	2,640	5.20	14	-76	12
5	L	Intracalcarine Cortex	2,408	4.37	-14	-76	12
6	R	Precentral Gyrus	2,352	5.54	12	-16	74
7	L	Lateral Occipital Cortex, inferior division	2,000	3.94	-48	-66	-18
7	L	Middle Temporal Gyrus, posterior division	2,000	3.64	-56	-42	-2
7	L	Middle Temporal Gyrus, temporooccipital part	2,000	4.30	-54	-50	4
7	L	Temporal Occipital Fusiform Cortex	2,000	4.20	-42	-60	-12
8	L	Precentral Gyrus	768	5.30	-32	-12	56
9	L	Superior Frontal Gyrus	624	5.07	-10	6	66

Supplemental Table 8. Descriptive statistics for clusters and local extrema showing greater activity during the Presentation of Threat relative to Safety (p<0.05, whole-brain-corrected for cluster extent p<0.001).

Cluster	**Left / Right**	**Label**	**mm³**	***t***	**x**	**y**	**z**
1	L	Intracalcarine Cortex	54,808	7.60	-16	-70	6
1	L	Lateral Occipital Cortex, inferior division	54,808	5.06	-40	-72	-8
1	L	Occipital Fusiform Gyrus	54,808	5.21	-34	-68	-18
1	L	Occipital Pole	54,808	5.96	-4	-100	-2
1	L	Temporal Occipital Fusiform Cortex	54,808	4.88	-32	-56	-16
1	R	Cuneal Cortex	54,808	4.56	18	-74	30
1	R	Intracalcarine Cortex	54,808	6.73	14	-66	10
1	R	Lateral Occipital Cortex, inferior division	54,808	4.75	36	-86	-10
1	R	Lingual Gyrus	54,808	6.55	4	-88	-2
1	R	Occipital Fusiform Gyrus	54,808	6.23	36	-68	-14
1	R	Occipital Pole	54,808	7.00	4	-90	4
1	R	Precuneus Cortex	54,808	5.64	18	-72	38
1	R	Temporal Fusiform Cortex, posterior division	54,808	4.05	36	-36	-24
1	R	Temporal Occipital Fusiform Cortex	54,808	5.82	36	-54	-14
2	R	Planum Temporale	10,504	5.35	38	-32	14
2	R	Superior Temporal Gyrus, posterior division	10,504	6.50	50	-16	-6
2	R	Supramarginal Gyrus, posterior division	10,504	4.75	68	-38	16
3	L	Central Opercular Cortex	7,128	3.51	-62	-14	10

3	L	Heschls Gyrus (includes H1 and H2)	7,128	4.75	-44	-24	8
3	L	Planum Temporale	7,128	5.77	-38	-34	10
3	L	Supramarginal Gyrus, posterior division	7,128	4.28	-66	-42	18
4	L	Frontal Orbital Cortex	3,264	5.07	-28	14	-18
4	L	Left Putamen	3,264	4.81	-22	8	-8
5	L	Cingulate Gyrus, posterior division	2,832	5.51	-2	-16	40
5	R	Cingulate Gyrus, posterior division	2,832	5.49	6	-24	28
6	R	Temporal Pole	2,816	5.44	54	8	-16
7	L	Brain-Stem	2,256	5.05	-6	-36	-6
7	R	Brain-Stem	2,256	4.51	12	-26	-10
8	L	Left Caudate	1,992	3.60	-8	8	14
9	L	Frontal Pole	1,416	4.24	-6	58	18
10	R	Frontal Orbital Cortex	1,400	4.93	32	18	-20
10	R	Right Putamen	1,400	4.47	26	12	-6
11	R	Precentral Gyrus	1,200	5.15	52	-2	48
12	L	Inferior Frontal Gyrus, pars opercularis	800	3.98	-48	20	10

Supplemental Table 9. Descriptive statistics for clusters and local extrema showing greater activity during the Presentation of Safety relative to Threat (p<0.05, whole-brain-corrected for cluster extent p<0.001).

Cluster	**Left / Right**	**Label**	**mm³**	***t***	**x**	**y**	**z**
1	L	Angular Gyrus	8,464	3.85	-44	-60	24
1	L	Lateral Occipital Cortex, superior division	8,464	6.42	-42	-78	30
2	L	Middle Frontal Gyrus	6,680	3.94	-38	10	62
2	L	Superior Frontal Gyrus	6,680	5.44	-24	14	60
3	L	Precuneus Cortex	5,968	6.86	-6	-54	16
3	R	Precuneus Cortex	5,968	4.82	8	-54	6
4	L	Cingulate Gyrus, posterior division	4,576	5.38	-6	-38	36
4	L	Precuneus Cortex	4,576	4.74	-2	-54	48
4	R	Lateral Occipital Cortex, superior division	4,576	3.84	12	-60	60
4	R	Precuneus Cortex	4,576	5.40	10	-60	50
4	R	Superior Parietal Lobule	4,576	3.80	12	-54	66
5	R	Lateral Occipital Cortex, superior division	2,920	6.61	46	-70	34
6	L	Lateral Occipital Cortex, superior division	2,896	4.55	-8	-64	62
6	L	Postcentral Gyrus	2,896	3.99	-8	-48	70
6	L	Precuneus Cortex	2,896	4.23	-8	-66	56
7	L	Middle Temporal Gyrus, temporooccipital part	2,208	5.62	-58	-50	-6
8	L	Parahippocampal Gyrus, posterior division	2,128	5.20	-28	-30	-18
8	L	Temporal Fusiform Cortex, posterior division	2,128	5.83	-26	-38	-18

9	R	Frontal Pole	1,232	4.12	28	36	50
9	R	Superior Frontal Gyrus	1,232	4.11	22	30	42
10	R	Middle Frontal Gyrus	1,000	3.96	26	16	54

Supplemental Table 10. Descriptive statistics for clusters and local extrema showing greater activity during the Presentation of Uncertain Safety relative to Certain Safety (p<0.05, whole-brain-corrected for cluster extent p<0.001).

Cluster	Left / Right	Label	mm³	*t*	x	y	z
1	L	Inferior Temporal Gyrus, temporooccipital part	6,664	5.96	-42	-54	-8
1	L	Lateral Occipital Cortex, inferior division	6,664	4.84	-40	-70	-6
1	L	Temporal Occipital Fusiform Cortex	6,664	5.78	-34	-48	-16
2	L	Superior Frontal Gyrus	4,200	4.29	-4	36	46
2	R	Cingulate Gyrus, anterior division	4,200	3.60	6	16	34
2	R	Juxtapositional Lobule Cortex	4,200	3.93	0	6	48
2	R	Paracingulate Gyrus	4,200	4.90	8	18	44
3	L	Occipital Pole	4,176	3.69	-2	-90	26
3	L	Precuneus Cortex	4,176	4.23	-10	-68	42
3	R	Lateral Occipital Cortex, superior division	4,176	3.52	10	-84	44
3	R	Occipital Pole	4,176	4.80	18	-98	24
3	R	Precuneus Cortex	4,176	3.62	4	-76	48
4	R	Superior Parietal Lobule	3,424	4.58	30	-42	42
4	R	Supramarginal Gyrus, posterior division	3,424	4.98	48	-38	48
5	R	Lateral Occipital Cortex, inferior division	2,696	3.37	40	-78	-12
5	R	Temporal Occipital Fusiform Cortex	2,696	5.23	36	-48	-18
6	R	Precuneus Cortex	2,504	5.06	10	-72	36
7	L	Precentral Gyrus	2,328	4.54	-48	0	36
8	R	Frontal Operculum Cortex	1,424	4.61	48	12	0
8	R	Insular Cortex	1,424	4.20	34	20	6
9	L	Frontal Operculum Cortex	1,344	3.83	-40	14	2
9	L	Insular Cortex	1,344	4.81	-30	18	10
10	R	Precentral Gyrus	1,176	4.55	48	6	32

Supplemental Table 11. Descriptive statistics for clusters and local extrema showing greater activity during the Presentation of Certain Safety relative to Uncertain Safety (p<0.05, whole-brain-corrected for cluster extent p<0.001).

Cluster	Left / Right	Label	mm³	*t*	x	y	z
1	R	Planum Temporale	2,640	4.60	58	-16	4
1	R	Superior Temporal Gyrus, anterior division	2,640	4.17	62	0	-6

1	R	Superior Temporal Gyrus, posterior division	2,640	4.61	68	-22	4
2	L	Heschls Gyrus (includes H1 and H2)	2,008	4.81	-52	-18	4
2	L	Planum Temporale	2,008	3.90	-62	-18	4
2	L	Superior Temporal Gyrus, anterior division	2,008	4.43	-62	-6	-6
2	L	Superior Temporal Gyrus, posterior division	2,008	4.40	-64	-12	2
3	L	Frontal Medial Cortex	1,104	4.75	-8	42	-12
3	L	Frontal Pole	1,104	4.38	-6	58	-16
3	R	Frontal Medial Cortex	1,104	4.05	0	42	-16

Supplemental Table 12. Descriptive statistics for clusters and local extrema showing the interaction between presentation conditions of Valence (Threat/Safety) and Temporal Certainty (Uncertain/Certain; $p<0.05$, whole-brain-corrected for cluster extent $p<0.001$), wherein a positive *t* statistic indicates: (Uncertain Threat – Certain Threat) > (Uncertain Safety – Certain Safety).

Cluster	**Left / Right**	**Label**	**mm³**	***t***	**x**	**y**	**z**
1	L	Lateral Occipital Cortex, superior division	5,160	5.18	-14	-66	60
1	L	Precuneus Cortex	5,160	5.26	-8	-64	52
1	R	Precuneus Cortex	5,160	5.36	10	-58	56
2	L	Pregenual anterior cingulate cortex	4,408	4.53	-2	38	12
2	R	Pregenual anterior cingulate cortex	4,408	4.81	4	36	14
2	R	Frontal Medial Cortex	4,408	4.57	10	50	-8
2	R	Frontal Pole/Dorsolateral Prefrontal Cortex	4,408	4.38	8	58	8
2	R	Paracingulate Gyrus	4,408	3.54	6	34	-10
3	L	Postcentral Gyrus	4,272	4.40	-50	-20	36
3	L	Supramarginal Gyrus, anterior division	4,272	5.21	-62	-30	32
4	L	Precuneus Cortex	1,912	4.75	-16	-68	24
5	R	Angular Gyrus	1,416	5.02	50	-54	14
6	L	Central Opercular Cortex	1,336	3.58	-44	6	0
6	L	Insular Cortex	1,336	4.80	-38	-8	-10
7	L	Frontal Medial Cortex	984	4.73	-10	48	-10
7	L	Frontal Pole/Dorsolateral Prefrontal Cortex	984	3.96	-4	58	0
8	L	Inferior Frontal Gyrus, pars opercularis	896	4.92	-58	10	18
8	L	Precentral Gyrus	896	4.22	-58	6	28
9	R	Brain-Stem	872	4.24	12	-16	-22
9	R	Parahippocampal Gyrus, anterior division	872	4.26	18	-16	-24
9	R	Right Hippocampus	872	4.43	26	-22	-18
9	R	Temporal Fusiform Cortex, posterior division	872	3.45	34	-22	-24

Supplemental Table 13. Descriptive statistics for clusters and local extrema showing the interaction between presentation conditions of Valence (Threat/Safety) and Temporal Certainty (Uncertain/Certain; $p<0.05$, whole-brain-corrected for cluster extent $p<0.001$), wherein a positive *t* statistic indicates: (Uncertain Threat – Certain Threat) < (Uncertain Safety – Certain Safety).

Cluster	Left / Right	Label	mm³	*t*	x	y	z
1	L	Intracalcarine Cortex	65,456	12.80	-16	-72	6
1	L	Lingual Gyrus	65,456	8.43	-18	-68	-4
1	L	Occipital Pole	65,456	7.24	-6	-98	-4
1	L	Cuneal Cortex	65,456	6.62	-2	-88	34
2	R	Intracalcarine Cortex	65,456	12.58	18	-68	8
1	R	Lingual Gyrus	65,456	11.50	0	-88	-4
1	R	Supracalcarine Cortex	65,456	11.24	2	-74	12
1	R	Cuneal Cortex	65,456	7.38	8	-84	36
1	R	Occipital Pole	65,456	7.09	12	-104	2

Supplemental Table 14. Descriptive statistics for clusters and local extrema showing greater activity during the Presentation of Uncertain Threat relative to Certain Threat ($p<0.05$, whole-brain-corrected for cluster extent $p<0.001$, pairwise contrasts masked by interaction between Valence and Temporal Certainty conditions).

Cluster	Left / Right	Label	mm³	*t*	x	y	z
1	L	Postcentral Gyrus	1,640	4.04	-50	-20	34
1	L	Supramarginal Gyrus, anterior division	1,640	4.69	-62	-28	34
2	R	Pregenual anterior cingulate cortex	840	4.95	6	38	14
3	L	Precentral Gyrus	816	5.15	-58	8	16
4	L	Lateral Occipital Cortex, superior division	696	3.62	-14	-68	56
5	L	Precuneus Cortex	672	4.74	-16	-66	24
6	L	Central Opercular Cortex	312	3.57	-48	8	0
6	L	Insular Cortex	312	4.76	-38	-8	-12

Supplemental Table 15. Descriptive statistics for clusters and local extrema showing greater activity during the Presentation of Uncertain Threat relative to Uncertain Safety ($p<0.05$, whole-brain-corrected for cluster extent $p<0.001$, pairwise contrasts masked by interaction between Valence and Temporal Certainty conditions).

Cluster	Left / Right	Label	mm³	*t*	x	y	z
1	L	Pregenual anterior cingulate cortex	1,752	5.04	-2	36	-4
1	R	Pregenual anterior cingulate cortex	1,752	4.66	6	40	10
2	L	Central Opercular Cortex	288	4.61	-62	-20	12
3	R	Frontal Pole/Dorsolateral Prefrontal Cortex	128	3.71	6	56	8

4	L	Supramarginal Gyrus, anterior division	120	3.31	-64	-38	24
5	L	Paracingulate Gyrus	40	3.64	-8	46	-2

Supplemental Table 16. Descriptive statistics for clusters and local extrema showing greater activity during the Presentation of Uncertain Threat relative to Certain Safety (p<0.05, whole-brain-corrected for cluster extent p<0.001, pairwise contrasts masked by interaction between Valence and Temporal Certainty conditions).

Cluster	Left / Right	Label	mm³	*t*	x	y	z
1	R	Brain-Stem	8	3.60	10	-18	-20
2	L	Precentral Gyrus	8	3.28	-58	6	32

Supplemental Table 17. Descriptive statistics for clusters and local extrema showing greater activity during the Presentation of Uncertain Safety relative to Certain Threat (p<0.05, whole-brain-corrected for cluster extent p<0.001, pairwise contrasts masked by interaction between Valence and Temporal Certainty conditions).

Cluster	Left / Right	Label	mm³	*t*	x	y	z
1	L	Precuneus Cortex	968	4.97	-12	-64	26
2	R	Precuneus Cortex	712	4.33	8	-58	52
3	L	Precuneus Cortex	8	3.32	-2	-62	18

Supplemental Table 18. Descriptive statistics for clusters and local extrema showing greater activity during the Presentation of Certain Safety relative to Uncertain Threat (p<0.05, whole-brain-corrected for cluster extent p<0.001, pairwise contrasts masked by interaction between Valence and Temporal Certainty conditions).

Cluster	Left / Right	Label	mm³	*t*	x	y	z
1	L	Precuneus Cortex	648	5.57	-6	-56	16
2	L	Lateral Occipital Cortex, superior division	408	4.06	-16	-66	64
3	L	Frontal Medial Cortex	64	4.51	-6	46	-12
4	L	Precuneus Cortex	8	3.30	-8	-66	22

Supplemental Table 19. Descriptive statistics for clusters and local extrema showing greater activity during the Presentation of Certain Safety relative to Certain Threat (p<0.05, whole-brain-corrected for cluster extent p<0.001, pairwise contrasts masked by interaction between Valence and Temporal Certainty conditions).

Cluster	Left / Right	Label	mm³	*t*	x	y	z
1	L	Lateral Occipital Cortex, superior division	5,104	6.24	-12	-64	60
1	L	Precuneus Cortex	5,104	6.21	-2	-56	48
1	R	Precuneus Cortex	5,104	6.47	10	-60	52
2	L	Postcentral Gyrus	2,440	4.31	-58	-24	40

2	L	Supramarginal Gyrus, anterior division	2,440	5.34	-62	-28	32
3	L	Precuneus Cortex	1,840	7.28	-6	-54	18
4	R	Parahippocampal Gyrus, anterior division	744	5.45	18	-16	-24
4	R	Right Hippocampus	744	6.18	26	-20	-18
5	L	Frontal Medial Cortex	472	4.19	-8	48	-10
5	L	Frontal Pole/Dorsolateral Prefrontal Cortex	472	3.61	-4	56	-2
5	R	Frontal Medial Cortex	472	3.69	0	52	-8
6	R	Frontal Medial Cortex	336	4.66	10	54	-8
7	R	Angular Gyrus	184	3.94	44	-56	22
8	R	Paracingulate Gyrus	8	3.25	8	42	-10

Supplemental Table 20. Descriptive statistics for clusters and local extrema showing greater activity during the Presentation of Certain Safety relative to Uncertain Safety (p<0.05, whole-brain-corrected for cluster extent p<0.001, pairwise contrasts masked by interaction between Valence and Temporal Certainty conditions).

Cluster	**Left / Right**	**Label**	**mm³**	***t***	**x**	**y**	**z**
1	L	Lateral Occipital Cortex, superior division	1,248	4.76	-14	-66	62
1	L	Precuneus Cortex	1,248	3.77	-8	-58	62
2	R	Pregenual anterior cingulate cortex	1,040	4.02	6	40	-2
2	R	Frontal Medial Cortex	1,040	5.05	10	50	-8
3	L	Frontal Medial Cortex	984	5.88	-6	48	-12
4	R	Angular Gyrus	816	4.52	52	-56	16
5	L	Precuneus Cortex	688	4.35	-8	-56	10
6	R	Precuneus Cortex	632	4.38	12	-58	58
7	L	Central Opercular Cortex	232	3.97	-62	-18	14
8	R	Frontal Pole/Dorsolateral Prefrontal Cortex	152	4.14	10	62	0
9	L	Pregenual anterior cingulate cortex	104	4.13	-4	36	-6

References

Abend, R., Gold, A. L., Britton, J. C., Michalska, K. J., Shechner, T., Sachs, J. F., Winkler, A. M., Leibenluft, E., Averbeck, B. B., & Pine, D. S. (2020). Anticipatory threat responding: Associations with anxiety, development, and brain structure. *Biological Psychiatry*, *87*(10), 916-925. https://doi.org/10.1016/j.biopsych.2019.11.006

Ahrens, S., Wu, M. V., Furlan, A., Hwang, G., Paik, R., Li, H., Penzo, M. A., Tollkuhn, J., & Li, B. (2018). A central extended amygdala circuit that modulates anxiety. *The Journal of Neuroscience*, *38*(24), 5567-5583. https://doi.org/10.1523/jneurosci.0705-18.2018

Alheid, G., & Heimer, L. (1988). New perspectives in basal forebrain organization of special relevance for neuropsychiatric disorders: The striatopallidal, amygdaloid, and corticopetal components of substantia innominata. *Neuroscience*, *27*(1), 1-39. https://doi.org/10.1016/0306-4522(88)90217-5

Alvarez, R. P., Chen, G., Bodurka, J., Kaplan, R., & Grillon, C. (2011). Phasic and sustained fear in humans elicits distinct patterns of brain activity. *NeuroImage*, *55*(1), 389-400. https://doi.org/10.1016/j.neuroimage.2010.11.057

American Psychiatric Association. (2013). Diagnostic and statistical manual of mental disorders. https://doi.org/10.1176/appi.books.9780890425596

Andreatta, M., Glotzbach-Schoon, E., Mühlberger, A., Schulz, S. M., Wiemer, J., & Pauli, P. (2015). Initial and sustained brain responses to contextual conditioned anxiety in humans. *Cortex, 63*, 352-363. https://doi.org/10.1016/j.cortex.2014.09.014

Andrzejewski, J. A., Greenberg, T., & Carlson, J. M. (2019). Neural correlates of aversive anticipation: An activation likelihood estimate meta-analysis across multiple sensory modalities. *Cognitive, Affective, & Behavioral Neuroscience, 19*(6), 1379-1390. https://doi.org/10.3758/s13415-019-00747-7

Angst, J., Gamma, A., Neuenschwander, M., Ajdacic-Gross, V., Eich, D., Rössler, W., & Merikangas, K. R. (2005). Prevalence of mental disorders in the Zurich cohort study: A twenty year prospective study. *Epidemiologia e Psichiatria Sociale, 14*(2), 68-76. https://doi.org/10.1017/s1121189x00006278

Apps, M., Rushworth, M., & Chang, S. (2016). The anterior Cingulate gyrus and social cognition: Tracking the motivation of others. *Neuron*, *90*(4), 692-707. https://doi.org/10.1016/j.neuron.2016.04.018

Avants, B. B., Tustison, N. J., Song, G., Cook, P. A., Klein, A., & Gee, J. C. (2011). A reproducible evaluation of ANTs similarity metric performance in brain image registration. *NeuroImage, 54*(3), 2033-2044. https://doi.org/10.1016/j.neuroimage.2010.09.025

Avery, S. N., Clauss, J. A., & Blackford, J. U. (2015). The human BNST: Functional role in anxiety and addiction. *Neuropsychopharmacology*, *41*(1), 126-141. https://doi.org/10.1038/npp.2015.185

Bandelow, B., & Michaelis, S. (2015). Epidemiology of anxiety disorders in the 21st century. *Anxiety*, *17*(3), 327-335. https://doi.org/10.31887/dcns.2015.17.3/bbandelow

Beaton, E. A., Schmidt, L. A., Schulkin, J., & Hall, G. B. (2010). Neural correlates of implicit processing of facial emotions in shy adults. *Personality and Individual Differences*, *49*(7), 755-761. https://doi.org/10.1016/j.paid.2010.06.021

Beesdo, K., Lau, J. Y., Guyer, A. E., McClure-Tone, E. B., Monk, C. S., Nelson, E. E., ... & Pine, D. S. (2009). Common and distinct amygdala-function perturbations in depressed vs anxious adolescents. *Archives of general psychiatry*, *66*(3), 275-285.

Beesdo-Baum, K., & Knappe, S. (2012). Developmental epidemiology of anxiety disorders. *Child and Adolescent Psychiatric Clinics of North America*, *21*(3), 457-478. https://doi.org/10.1016/j.chc.2012.05.001

Birbaumer, N., & Flor, H. (1998). Psychobiology. *Comprehensive Clinical Psychology*, 115-172. https://doi.org/10.1016/b0080-4270(73)00218-2

Birk, S. L., Horenstein, A., Weeks, J., Olino, T., Heimberg, R., Goldin, P. R., & Gross, J. J. (2019). Neural responses to social evaluation: The role of fear of positive and negative evaluation. *Journal of anxiety disorders*, *67*, 102114.

Birn, R. M., Shackman, A. J., Oler, J. A., Williams, L. E., McFarlin, D. R., Rogers, G. M., Shelton, S. E., Alexander, A. L., Pine, D. S., Slattery, M. J., Davidson, R. J., Fox, A. S., & Kalin, N. H. (2014). Evolutionarily conserved prefrontal-amygdalar dysfunction in early-life anxiety. *Molecular Psychiatry*, *19*(8), 915-922. https://doi.org/10.1038/mp.2014.46

Boehme, S., Ritter, V., Tefikow, S., Stangier, U., Strauss, B., Miltner, W. H., & Straube, T. (2013). Brain activation during anticipatory anxiety in social anxiety disorder. *Social Cognitive and Affective Neuroscience*, *9*(9), 1413-1418. https://doi.org/10.1093/scan/nst129

Brinkmann, L., Buff, C., Neumeister, P., Tupak, S. V., Becker, M. P., Herrmann, M. J., & Straube, T. (2017). Dissociation between amygdala and bed nucleus of the stria terminalis during threat anticipation in female post-traumatic stress disorder patients. *Human Brain Mapping*, *38*(4), 2190-2205. https://doi.org/10.1002/hbm.23513

Brotman, M. A., Rich, B. A., Guyer, A. E., Lunsford, J. R., Horsey, S. E., Reising, M. M., ... & Leibenluft, E. (2010). Amygdala activation during emotion processing of neutral faces in children with severe mood dysregulation versus ADHD or bipolar disorder. *American Journal of Psychiatry*, *167*(1), 61-69.

Brühl, A. B., Delsignore, A., Komossa, K., & Weidt, S. (2014). Neuroimaging in social anxiety disorder—A meta-analytic review resulting in a new neurofunctional

model. *Neuroscience & Biobehavioral Reviews*, *47*, 260-280. https://doi.org/10.1016/j.neubiorev.2014.08.003

Buff, C., Schmidt, C., Brinkmann, L., Gathmann, B., Tupak, S., & Straube, T. (2017). Directed threat imagery in generalized anxiety disorder. *Psychological Medicine*, *48*(4), 617-628. https://doi.org/10.1017/s0033291717001957

Bunnell, B. E., Beidel, D. C., Liu, L., Joseph, D. L., & Higa-McMillan, C. (2015). The SPAIC-11 and SPAICP-11: Two brief child- and parent-rated measures of social anxiety. *Journal of Anxiety Disorders*, *36*, 103-109. https://doi.org/10.1016/j.janxdis.2015.10.002

Bögels, S. M., Alden, L., Beidel, D. C., Clark, L. A., Pine, D. S., Stein, M. B., & Voncken, M. (2010). Social anxiety disorder: Questions and answers for the DSM-V. *Depression and Anxiety*, *27*(2), 168-189. https://doi.org/10.1002/da.20670

Bögels, S. M., Alden, L., Beidel, D. C., Clark, L. A., Pine, D. S., Stein, M. B., & Voncken, M. (2010). Social anxiety disorder: Questions and answers for the DSM-V. *Depression and Anxiety*, *27*(2), 168-189. https://doi.org/10.1002/da.20670

Caouette, J. D., & Guyer, A. E. (2014). Gaining insight into adolescent vulnerability for social anxiety from developmental cognitive neuroscience. *Developmental Cognitive Neuroscience*, *8*, 65-76. https://doi.org/10.1016/j.dcn.2013.10.003

Carré, A., Gierski, F., Lemogne, C., Tran, E., Raucher-Chéné, D., Béra-Potelle, C., Portefaix, C., Kaladjian, A., Pierot, L., Besche-Richard, C., & Limosin, F. (2013). Linear association between social anxiety symptoms and neural activations to angry faces: From subclinical to clinical levels. *Social Cognitive and Affective Neuroscience*, *9*(6), 880-886. https://doi.org/10.1093/scan/nst061

Carskadon, M., & Acebo, C. (1993). Puberty development scale--adapted version. *PsycTESTS Dataset*. https://doi.org/10.1037/t23990-000

Cartwright-Hatton, S., McNicol, K., & Doubleday, E. (2006). Anxiety in a neglected population: Prevalence of anxiety disorders in pre-adolescent children. *Clinical Psychology Review*, *26*(7), 817-833. https://doi.org/10.1016/j.cpr.2005.12.002

Clark, D. M., & Wells, A. (1995). A cognitive model of social phobia. In R. G. Heimberg, M. R. Liebowitz, D. A. Hope, & F. R. Schneier (Eds.). *Social phobia: Diagnosis, Assessment, and Treatment*, 69-93.

Clauss, J. A., Avery, S. N., Benningfield, M. M., & Blackford, J. U. (2019). Social anxiety is associated with BNST response to unpredictability. *Depression and Anxiety*, *36*(8), 666-675. https://doi.org/10.1002/da.22891

Conway, C. C., Forbes, M. K., Forbush, K. T., Fried, E. I., Hallquist, M. N., Kotov, R., Mullins-Sweatt, S. N., Shackman, A. J., Skodol, A. E., South, S. C., Sunderland, M., Waszczuk, M. A., Zald, D. H., Afzali, M. H., Bornovalova, M. A., Carragher, N., Docherty, A. R., Jonas, K. G., Krueger, R. F., … Eaton, N. R. (2019). A hierarchical taxonomy of psychopathology can

transform mental health research. *Perspectives on Psychological Science*, *14*(3), 419-436. https://doi.org/10.1177/1745691618810696

Conway, C. C., Forbes, M. K., Forbush, K. T., Fried, E. I., Hallquist, M. N., Kotov, R., Mullins-Sweatt, S. N., Shackman, A. J., Skodol, A. E., South, S. C., Sunderland, M., Waszczuk, M. A., Zald, D. H., Afzali, M. H., Bornovalova, M. A., Carragher, N., Docherty, A. R., Jonas, K. G., Krueger, R. F., … Eaton, N. R. (2019). A hierarchical taxonomy of psychopathology can transform mental health research. *Perspectives on Psychological Science*, *14*(3), 419-436. https://doi.org/10.1177/1745691618810696

Cooney, R. E., Atlas, L. Y., Joormann, J., Eugène, F., & Gotlib, I. H. (2006). Amygdala activation in the processing of neutral faces in social anxiety disorder: Is neutral really neutral? *Psychiatry Research: Neuroimaging*, *148*(1), 55-59. https://doi.org/10.1016/j.pscychresns.2006.05.003

Cox, R. W. (1996). AFNI: Software for analysis and visualization of functional magnetic resonance Neuroimages. *Computers and Biomedical Research*, *29*(3), 162-173. https://doi.org/10.1006/cbmr.1996.0014

Cox, R. W. (1996). AFNI: Software for analysis and visualization of functional magnetic resonance Neuroimages. *Computers and Biomedical Research*, *29*(3), 162-173. https://doi.org/10.1006/cbmr.1996.0014

Crane, N. A., Chang, F., Kinney, K. L., & Klumpp, H. (2021). Individual differences in striatal and amygdala response to emotional faces are related to symptom severity

in social anxiety disorder. *NeuroImage: Clinical*, *30*, 102615. https://doi.org/10.1016/j.nicl.2021.102615

Craske, M. G., Stein, M. B., Eley, T. C., Milad, M. R., Holmes, A., Rapee, R. M., & Wittchen, H. (2017). Correction: Anxiety disorders. *Nature Reviews Disease Primers*, *3*(1). https://doi.org/10.1038/nrdp.2017.100

Craske, M. G., Wolitzky-Taylor, K. B., Mineka, S., Zinbarg, R., Waters, A. M., Vrshek-Schallhorn, S., Epstein, A., Naliboff, B., & Ornitz, E. (2012). Elevated responding to safe conditions as a specific risk factor for anxiety versus depressive disorders: Evidence from a longitudinal investigation. *Journal of Abnormal Psychology*, *121*(2), 315-324. https://doi.org/10.1037/a0025738

Cremers, H. R., & Roelofs, K. (2016). Social anxiety disorder: A critical overview of neurocognitive research. *Wiley Interdisciplinary Reviews: Cognitive Science*, *7*(4), 218-232. https://doi.org/10.1002/wcs.1390

Cuthbert, B., & Insel, T. (2010). Classification issues in women's mental health: Clinical utility and etiological mechanisms. *Archives of Women's Mental Health*, *13*(1), 57-59. https://doi.org/10.1007/s00737-009-0132-z

Cuthbert, B., & Insel, T. (2010). The data of diagnosis: New approaches to psychiatric classification. *Psychiatry: Interpersonal and Biological Processes*, *73*(4), 311-314. https://doi.org/10.1521/psyc.2010.73.4.311

Cuthbert, B. N., & Insel, T. R. (2013). Toward the future of psychiatric diagnosis: The seven pillars of RDoC. *BMC Medicine*, *11*(1). https://doi.org/10.1186/1741-7015-11-126

Cuthbert, B. N., & Insel, T. R. (2013). Toward the future of psychiatric diagnosis: The seven pillars of RDoC. *BMC Medicine*, *11*(1). https://doi.org/10.1186/1741-7015-11-126

Daldrup, T., Remmes, J., Lesting, J., Gaburro, S., Fendt, M., Meuth, P., Kloke, V., Pape, H., & Seidenbecher, T. (2015). Expression of freezing and fear-potentiated startle during sustained fear in mice. *Genes, Brain and Behavior*, *14*(3), 281-291. https://doi.org/10.1111/gbb.12211

Davies, C. D., Young, K., Torre, J. B., Burklund, L. J., Goldin, P. R., Brown, L. A., Niles, A. N., Lieberman, M. D., & Craske, M. G. (2017). Altered time course of amygdala activation during speech anticipation in social anxiety disorder. *Journal of Affective Disorders*, *209*, 23-29. https://doi.org/10.1016/j.jad.2016.11.014

Davis, M., Walker, D. L., Miles, L., & Grillon, C. (2009). Phasic vs sustained fear in rats and humans: Role of the extended amygdala in fear vs anxiety. *Neuropsychopharmacology*, *35*(1), 105-135. https://doi.org/10.1038/npp.2009.109

Duits, P., Cath, D. C., Lissek, S., Hox, J. J., Hamm, A. O., Engelhard, I. M., Van den Hout, M. A., & Baas, J. M. (2015). Updated meta-analysis of classical fear conditioning in the anxiety disorders. *Depression and Anxiety*, *32*(4), 239-253. https://doi.org/10.1002/da.22353

Eldreth, D., Hardin, M. G., Pavletic, N., & Ernst, M. (2013). Adolescent transformations of behavioral and neural processes as potential targets for prevention. *Prevention Science, 14*(3), 257-266. https://doi.org/10.1007/s11121-012-0322-1

Eskildsen, S. F., Coupé, P., Fonov, V., Manjón, J. V., Leung, K. K., Guizard, N., Wassef, S. N., Østergaard, L. R., & Collins, D. L. (2012). BEaST: Brain extraction based on nonlocal segmentation technique. *NeuroImage, 59*(3), 2362-2373. https://doi.org/10.1016/j.neuroimage.2011.09.012

Etkin, A., & Wager, T. D. (2007). Functional neuroimaging of anxiety: A meta-analysis of emotional processing in PTSD, social anxiety disorder, and specific phobia. *American Journal of Psychiatry, 164*(10), 1476-1488. https://doi.org/10.1176/appi.ajp.2007.07030504

Ezpeleta, L., Keeler, G., Erkanli, A., Costello, E. J., & Angold, A. (2001). Epidemiology of psychiatric disability in childhood and adolescence. *Journal of Child Psychology and Psychiatry, 42*(7), 901-914. https://doi.org/10.1111/1469-7610.00786

Ferri, J., Bress, J. N., Eaton, N. R., & Proudfit, G. H. (2014). The impact of puberty and social anxiety on amygdala activation to faces in adolescence. *Developmental Neuroscience, 36*(3-4), 239-249.

Figel, B., Brinkmann, L., Buff, C., Heitmann, C. Y., Hofmann, D., Bruchmann, M., Becker, M. P., Herrmann, M. J., & Straube, T. (2019). Phasic amygdala and BNST activation during the anticipation of temporally unpredictable social

observation in social anxiety disorder patients. *NeuroImage: Clinical*, *22*, 101735. https://doi.org/10.1016/j.nicl.2019.101735

Filkowski, M., Cochran, R. N., & Haas, B. (2017). Altruistic behavior: Mapping responses in the brain. *Neuroscience and Neuroeconomics*, *5*, 65-75. https://doi.org/10.2147/nan.s87718

Fox, A. S., Oler, J. A., Tromp, D. P., Fudge, J. L., & Kalin, N. H. (2015). Extending the amygdala in theories of threat processing. *Trends in Neurosciences*, *38*(5), 319-329. https://doi.org/10.1016/j.tins.2015.03.002

Fox, A. S., & Shackman, A. J. (2019). The central extended amygdala in fear and anxiety: Closing the gap between mechanistic and neuroimaging research. *Neuroscience Letters*, *693*, 58-67. https://doi.org/10.1016/j.neulet.2017.11.056

Fredrick, J. W., & Luebbe, A. M. (2020). Fear of positive evaluation and social anxiety: A systematic review of trait-based findings. *Journal of Affective Disorders*, *265*, 157-168. https://doi.org/10.1016/j.jad.2020.01.042

Garrett, A. S., Carrion, V., Kletter, H., Karchemskiy, A., Weems, C. F., & Reiss, A. (2012). Brain activation to facial expressions in youth with PTSD symptoms. *Depression and Anxiety*, *29*(5), 449-459.

Gentili, C., Cristea, I. A., Angstadt, M., Klumpp, H., Tozzi, L., Phan, K. L., & Pietrini, P. (2015). Beyond emotions: A meta-analysis of neural response within face

processing system in social anxiety. *Experimental Biology and Medicine*, *241*(3), 225-237. https://doi.org/10.1177/1535370215603514

Gentili, C., Gobbini, M., Ricciardi, E., Vanello, N., Pietrini, P., Haxby, J., & Guazzelli, M. (2008). Imbalanced activation of the distributed neural system for face perception in social phobia. *International Journal of Psychophysiology*, *69*(3), 225. https://doi.org/10.1016/j.ijpsycho.2008.05.070

Gold, A. L., Abend, R., Britton, J. C., Behrens, B., Farber, M., Ronkin, E., ... & Pine, D. S. (2020). Age differences in the neural correlates of anxiety disorders: An fMRI study of response to learned threat. *American Journal of Psychiatry*, *177*(5), 454-463.

Gorka, S. M., Lieberman, L., Shankman, S. A., & Phan, K. L. (2017). Association between neural reactivity and startle reactivity to uncertain threat in two independent samples. *Psychophysiology*, *54*(5), 652-662. https://doi.org/10.1111/psyp.12829

Gothard, K. M. (2020). Multidimensional processing in the amygdala. *Nature Reviews Neuroscience*, *21*(10), 565-575. https://doi.org/10.1038/s41583-020-0350-y

Gregory, A. M., Caspi, A., Moffitt, T. E., Koenen, K., Eley, T. C., & Poulton, R. (2007). Juvenile mental health histories of adults with anxiety disorders. *American Journal of Psychiatry*, *164*(2), 301-308. https://doi.org/10.1176/ajp.2007.164.2.301

Greve, D. N., & Fischl, B. (2009). Accurate and robust brain image alignment using boundary-based registration. *NeuroImage*, *48*(1), 63-72. https://doi.org/10.1016/j.neuroimage.2009.06.060

Grupe, D. W., & Nitschke, J. B. (2013). Uncertainty and anticipation in anxiety: An integrated neurobiological and psychological perspective. *Nature Reviews Neuroscience*, *14*(7), 488-501. https://doi.org/10.1038/nrn3524

Grupe, D. W., Wielgosz, J., Davidson, R. J., & Nitschke, J. B. (2016). Neurobiological correlates of distinct post-traumatic stress disorder symptom profiles during threat anticipation in combat veterans. *Psychological Medicine*, *46*(9), 1885-1895. https://doi.org/10.1017/s0033291716000374

Gungor, N. Z., & Pare, D. (2016). Functional heterogeneity in the bed nucleus of the stria Terminalis. *Journal of Neuroscience*, *36*(31), 8038-8049. https://doi.org/10.1523/jneurosci.0856-16.2016

Haller, S. P., Cohen Kadosh, K., Scerif, G., & Lau, J. Y. (2015). Social anxiety disorder in adolescence: How developmental cognitive neuroscience findings may shape understanding and interventions for psychopathology. *Developmental Cognitive Neuroscience*, *13*, 11-20. https://doi.org/10.1016/j.dcn.2015.02.002

Hattingh, C. J., Ipser, J., Tromp, S. A., Syal, S., Lochner, C., Brooks, S. J., & Stein, D. J. (2013). Functional magnetic resonance imaging during emotion recognition in social anxiety disorder: An activation likelihood meta-analysis. *Frontiers in Human Neuroscience*, *6*. https://doi.org/10.3389/fnhum.2012.00347

Hefner, K. R., Moberg, C. A., Hachiya, L. Y., & Curtin, J. J. (2013). Alcohol stress response dampening during imminent versus distal, uncertain threat. *Journal of Abnormal Psychology*, *122*(3), 756-769. https://doi.org/10.1037/a0033407

Heimberg, R. G., Hofmann, S. G., Liebowitz, M. R., Schneier, F. R., Smits, J. A., Stein, M. B., Hinton, D. E., & Craske, M. G. (2014). Social anxiety disorder in DSM-5. *Depression and Anxiety*, *31*(6), 472-479. https://doi.org/10.1002/da.22231

Heitmann, C. Y., Feldker, K., Neumeister, P., Brinkmann, L., Schrammen, E., Zwitserlood, P., & Straube, T. (2017). Brain activation to task-irrelevant disorder-related threat in social anxiety disorder: The impact of symptom severity. *NeuroImage: Clinical*, *14*, 323-333. https://doi.org/10.1016/j.nicl.2017.01.020

Herrmann, M. J., Boehme, S., Becker, M. P., Tupak, S. V., Guhn, A., Schmidt, B., Brinkmann, L., & Straube, T. (2016). Phasic and sustained brain responses in the amygdala and the bed nucleus of the stria terminalis during threat anticipation. *Human Brain Mapping*, *37*(3), 1091-1102. https://doi.org/10.1002/hbm.23088

Hofmann, S. G. (2007). Cognitive factors that maintain social anxiety disorder: A comprehensive model and its treatment implications. *Cognitive Behaviour Therapy*, *36*(4), 193-209. https://doi.org/10.1080/16506070701421313

Hur, J., Smith, J. F., DeYoung, K. A., Anderson, A. S., Kuang, J., Kim, H. C., Tillman, R. M., Kuhn, M., Fox, A. S., & Shackman, A. J. (2020). Anxiety and the

neurobiology of temporally uncertain threat anticipation. https://doi.org/10.1101/2020.02.25.964734

Hur, J., Tillman, R. M., Fox, A. S., & Shackman, A. J. (2019). The value of clinical and translational neuroscience approaches to psychiatric illness. *Behavioral and Brain Sciences, 42*, e11.

Im, H. Y., Adams Jr, R. B., Cushing, C. A., Boshyan, J., Ward, N., & Kveraga, K. (2018). Sex-related differences in behavioral and amygdalar responses to compound facial threat cues. *Human Brain Mapping*, *39*(7), 2725-2741.

James, A. C., James, G., Cowdrey, F. A., Soler, A., & Choke, A. (2013). Cognitive behavioural therapy for anxiety disorders in children and adolescents. *Cochrane Database of Systematic Reviews*. https://doi.org/10.1002/14651858.cd004690.pub3

Jarcho, J. M., Leibenluft, E., Walker, O. L., Fox, N. A., Pine, D. S., & Nelson, E. E. (2013). Neuroimaging studies of pediatric social anxiety: Paradigms, pitfalls and a new direction for investigating the neural mechanisms. *Biology of Mood & Anxiety Disorders*, *3*(1). https://doi.org/10.1186/2045-5380-3-14

Kaczkurkin, A. N., Moore, T. M., Ruparel, K., Ciric, R., Calkins, M. E., Shinohara, R. T., ... & Satterthwaite, T. D. (2016). Elevated amygdala perfusion mediates developmental sex differences in trait anxiety. *Biological Psychiatry*, *80*(10), 775-785.

Kaufman, J., Birmaher, B., Brent, D., Rao, U., Flynn, C., Moreci, P., Williamson, D., & Ryan, N. (1997). Schedule for affective disorders and schizophrenia for school-age children-present and lifetime version. *PsycTESTS Dataset*. https://doi.org/10.1037/t03988-000

Kessler, R. C., Berglund, P., Demler, O., Jin, R., Merikangas, K. R., & Walters, E. E. (2005). Lifetime prevalence and age-of-Onset distributions of DSM-IV disorders in the national comorbidity survey replication. *Archives of General Psychiatry, 62*(6), 593. https://doi.org/10.1001/archpsyc.62.6.593

Kessler, R. C., Petukhova, M., Sampson, N. A., Zaslavsky, A. M., & Wittchen, H. (2012). Twelve-month and lifetime prevalence and lifetime morbid risk of anxiety and mood disorders in the United States. *International Journal of Methods in Psychiatric Research*, *21*(3), 169-184. https://doi.org/10.1002/mpr.1359

Klein, A., Andersson, J., Ardekani, B. A., Ashburner, J., Avants, B., Chiang, M., Christensen, G. E., Collins, D. L., Gee, J., Hellier, P., Song, J. H., Jenkinson, M., Lepage, C., Rueckert, D., Thompson, P., Vercauteren, T., Woods, R. P., Mann, J. J., & Parsey, R. V. (2009). Evaluation of 14 nonlinear deformation algorithms applied to human brain MRI registration. *NeuroImage, 46*(3), 786-802. https://doi.org/10.1016/j.neuroimage.2008.12.037

Klumpers, F., Kroes, M. C., Heitland, I., Everaerd, D., Akkermans, S. E., Oosting, R. S., Van Wingen, G., Franke, B., Kenemans, J. L., Fernández, G., & Baas, J. M. (2015). Dorsomedial prefrontal cortex mediates the impact of serotonin

transporter linked polymorphic region genotype on anticipatory threat reactions. *Biological Psychiatry, 78*(8), 582-589. https://doi.org/10.1016/j.biopsych.2014.07.034

Klumpers, F., Kroes, M. C., Baas, J. M., & Fernández, G. (2017). How human amygdala and bed nucleus of the stria Terminalis may drive distinct defensive responses. *The Journal of Neuroscience, 37*(40), 9645-9656. https://doi.org/10.1523/jneurosci.3830-16.2017

Knight, A., McLellan, L., Jones, M., & Hudson, J. (2014). Pre-treatment predictors of outcome in childhood anxiety disorders: A systematic review. *Psychopathology Review*, *a1*(1), 77-129. https://doi.org/10.5127/pr.034613

Kotov, R., Krueger, R., Watson, D., Achenbach, T., Althoff, R., Bagby, M., Brown, T., Docherty, A., Miller, J., Simms, L., South, S. C., & Tackett, J. L. (2017). The hierarchical taxonomy of psychopathology (HiTOP): A dimensional alternative to traditional Nosologies. https://doi.org/10.31234/osf.io/zaadn

Krüger, O., Shiozawa, T., Kreifelts, B., Scheffler, K., & Ethofer, T. (2015). Three distinct fiber pathways of the bed nucleus of the stria terminalis to the amygdala and prefrontal cortex. *Cortex, 66*, 60-68. https://doi.org/10.1016/j.cortex.2015.02.007

Lange, M. D., Daldrup, T., Remmers, F., Szkudlarek, H. J., Lesting, J., Guggenhuber, S., Ruehle, S., Jüngling, K., Seidenbecher, T., Lutz, B., & Pape, H. C. (2017). Cannabinoid CB1 receptors in distinct circuits of the extended amygdala

determine fear responsiveness to unpredictable threat. *Molecular Psychiatry, 22*(10), 1422-1430. https://doi.org/10.1038/mp.2016.156

Latzman, R. D., DeYoung, C. G., Afzali, M. H., Allen, T. A., Althoff, R. R., Docherty, A. R., . . . The Hitop Neurobiological Foundations Workgroup. (2020). Using empirically-derived dimensional phenotypes to accelerate clinical neuroscience: the Hierarchical Taxonomy of Psychopathology (HiTOP) framework. *Neuropsychopharmacology, 45*, 1083-1085.

Lebow, M. A., & Chen, A. (2016). Overshadowed by the amygdala: the bed nucleus of the stria terminalis emerges as key to psychiatric disorders. *Molecular Psychiatry*, *21*(4), 450-463.

LeDoux, J. E., & Pine, D. S. (2016). Using neuroscience to help understand fear and anxiety: A two-system framework. *American Journal of Psychiatry*, *173*(11), 1083-1093. https://doi.org/10.1176/appi.ajp.2016.16030353

Leigh, E., & Clark, D. M. (2018). Understanding social anxiety disorder in adolescents and improving treatment outcomes: Applying the cognitive model of Clark and Wells (1995). *Clinical Child and Family Psychology Review*, *21*(3), 388-414. https://doi.org/10.1007/s10567-018-0258-5

Lorberbaum JP, Kose S, Johnson MR, Arana GW, Sullivan LK, Hamner MB, et al. Neural correlates of speech anticipatory anxiety in generalized social phobia. Neuroreport. 2004;15:2701–2705.

Lorio, S., Fresard, S., Adaszewski, S., Kherif, F., Chowdhury, R., Frackowiak, R., Ashburner, J., Helms, G., Weiskopf, N., Lutti, A., & Draganski, B. (2016). New tissue priors for improved automated classification of subcortical brain structures on MRI. *NeuroImage*, *130*, 157-166. https://doi.org/10.1016/j.neuroimage.2016.01.062

Ma, D. S., Correll, J., & Wittenbrink, B. (2015). The Chicago face database: A free stimulus set of faces and norming data. *Behavior Research Methods*, *47*(4), 1122-1135. https://doi.org/10.3758/s13428-014-0532-5

Mai, J. K., Paxinos, G., & Voss, T. (2007). *Atlas of the human brain*. Academic Press.

McClure, E. B., Monk, C. S., Nelson, E. E., Zarahn, E., Leibenluft, E., Bilder, R. M., ... & Pine, D. S. (2004). A developmental examination of gender differences in brain engagement during evaluation of threat. *Biological Psychiatry*, *55*(11), 1047-1055.

McFarquhar, M., McKie, S., Emsley, R., Suckling, J., Elliott, R., & Williams, S. (2016). Multivariate and repeated measures (MRM): A new toolbox for dependent and multimodal group-level neuroimaging data. Neuroimage, 132, 373-389.

Merikangas, K. R., Avenevoli, S., Acharyya, S., Zhang, H., & Angst, J. (2002). The spectrum of social phobia in the Zurich cohort study of young adults. *Biological Psychiatry*, *51*(1), 81-91. https://doi.org/10.1016/s0006-3223(01)01309-9

Merikangas, K. R., Avenevoli, S., Acharyya, S., Zhang, H., & Angst, J. (2002). The spectrum of social phobia in the Zurich cohort study of young adults. *Biological Psychiatry*, *51*(1), 81-91. https://doi.org/10.1016/s0006-3223(01)01309-9

Miles, L., Davis, M., & Walker, D. (2011). Phasic and sustained fear are pharmacologically dissociable in rats. *Neuropsychopharmacology*, *36*(8), 1563-1574. https://doi.org/10.1038/npp.2011.29

Miskovic, V., & Schmidt, L. A. (2012). Early information processing biases in social anxiety. *Cognition & Emotion*, *26*(1), 176-185. https://doi.org/10.1080/02699931.2011.565037

Mobbs, D., Yu, R., Rowe, J. B., Eich, H., FeldmanHall, O., & Dalgleish, T. (2010). Neural activity associated with monitoring the oscillating threat value of a tarantula. *Proceedings of the National Academy of Sciences*, *107*(47), 20582-20586. https://doi.org/10.1073/pnas.1009076107

Monk, C. S., Nelson, E. E., McClure, E. B., Mogg, K., Bradley, B. P., Leibenluft, E., ... & Pine, D. S. (2006). Ventrolateral prefrontal cortex activation and attentional bias in response to angry faces in adolescents with generalized anxiety disorder. *American Journal of Psychiatry*, *163*(6), 1091-1097.

Monk, C. S., Telzer, E. H., Mogg, K., Bradley, B. P., Mai, X., Louro, H. M., ... & Pine, D. S. (2008). Amygdala and ventrolateral prefrontal cortex activation to masked angry faces in children and adolescents with generalized anxiety disorder. *Archives of General Psychiatry*, *65*(5), 568-576.

Münsterkötter, A. L., Notzon, S., Redlich, R., Grotegerd, D., Dohm, K., Arolt, V., Kugel, H., Zwanzger, P., & Dannlowski, U. (2015). Spider or no spider? Neural correlates of sustained and phasic fear in spider phobia. *Depression and Anxiety, 32*(9), 656-663. https://doi.org/10.1002/da.22382

Nacewicz, B. M. , Alexander, A. L. , Kalin, N. H. , & Davidson, R. J. (2014). The neurochemical underpinnings of human amygdala volume including subregional contributions. Biological Psychiatry, 75, S222.

Najafi, M., Kinnison, J., & Pessoa, L. (2017). Intersubject brain networks during anxious anticipation. *Frontiers in Human Neuroscience*, *11*. https://doi.org/10.3389/fnhum.2017.00552

National Institute of Mental Health (2011) Negative valence systems: Workshop proceedings. Rockville, MD.

National Institute of Mental Health (2020a) Construct: potential threat ("anxiety"). Bethesda, MD: National Institute of Mental Health.

National Institute of Mental Health (2020b) Construct: acute threat ("fear"). Bethesda, MD: National Institute of Mental Health.

Norbury, A., Robbins, T. W., & Seymour, B. (2018). Author response: Value generalization in human avoidance learning. https://doi.org/10.7554/elife.34779.028

Oler, J. A., Birn, R. M., Patriat, R., Fox, A. S., Shelton, S. E., Burghy, C. A., Stodola, D. E., Essex, M. J., Davidson, R. J., & Kalin, N. H. (2012). Evidence for coordinated functional activity within the extended amygdala of non-human and human primates. *NeuroImage*, *61*(4), 1059-1066. https://doi.org/10.1016/j.neuroimage.2012.03.045

Oler, J. A., Tromp, D. P., Fox, A. S., Kovner, R., Davidson, R. J., Alexander, A. L., McFarlin, D. R., Birn, R. M., E. Berg, B., DeCampo, D. M., Kalin, N. H., & Fudge, J. L. (2017). Connectivity between the central nucleus of the amygdala and the bed nucleus of the stria terminalis in the non-human primate: Neuronal tract tracing and developmental neuroimaging studies. *Brain Structure and Function*, *222*(1), 21-39. https://doi.org/10.1007/s00429-016-1198-9

Pedersen, W. S., Muftuler, L. T., & Larson, C. L. (2019). A high-resolution fMRI investigation of BNST and centromedial amygdala activity as a function of affective stimulus predictability, anticipation, and duration. *Social Cognitive and Affective Neuroscience*, *14*(11), 1167-1177. https://doi.org/10.1093/scan/nsz095

Pessoa, L., & Padmala, S. (2005). Quantitative prediction of perceptual decisions during near-threshold fear detection. *Proceedings of the National Academy of Sciences*, *102*(15), 5612-5617.

Petersen, A. C., Crockett, L., Richards, M., & Boxer, A. (1988). Pubertal development scale. *PsycTESTS Dataset*. https://doi.org/10.1037/t06349-000

Pittig, A., Treanor, M., LeBeau, R. T., & Craske, M. G. (2018). The role of associative fear and avoidance learning in anxiety disorders: Gaps and directions for future research. *Neuroscience & Biobehavioral Reviews*, *88*, 117-140. https://doi.org/10.1016/j.neubiorev.2018.03.015

Pruim, R. H., Mennes, M., Van Rooij, D., Llera, A., Buitelaar, J. K., & Beckmann, C. F. (2015). ICA-AROMA: A robust ICA-based strategy for removing motion artifacts from fMRI data. *NeuroImage*, *112*, 267-277. https://doi.org/10.1016/j.neuroimage.2015.02.064

Pujol, J., Harrison, B. J., Ortiz, H., Deus, J., Soriano-Mas, C., López-Solà, M., Yücel, M., Perich, X., & Cardoner, N. (2009). Influence of the fusiform gyrus on amygdala response to emotional faces in the non-clinical range of social anxiety. *Psychological Medicine*, *39*(07), 1177. https://doi.org/10.1017/s003329170800500x

Rapee, R. M., Oar, E. L., Johnco, C. J., Forbes, M. K., Fardouly, J., Magson, N. R., & Richardson, C. E. (2019). Adolescent development and risk for the onset of social-emotional disorders: A review and conceptual model. *Behaviour Research and Therapy*, *123*, 103501.

Reichenberger, J., Wiggert, N., Wilhelm, F. H., Liedlgruber, M., Voderholzer, U., Hillert, A., ... & Blechert, J. (2019). Fear of negative and positive evaluation and reactivity to social-evaluative videos in social anxiety disorder. Behaviour research and therapy, 116, 140-148.

Ressler, R. L., Goode, T. D., Evemy, C., & Maren, S. (2020). NMDA receptors in the Cea and BNST differentially regulate fear conditioning to predictable and unpredictable threats. *Neurobiology of Learning and Memory*, *174*, 107281. https://doi.org/10.1016/j.nlm.2020.107281

Rodebaugh, T. L., Weeks, J. W., Gordon, E. A., Langer, J. K., & Heimberg, R. G. (2012). The longitudinal relationship between fear of positive evaluation and fear of negative evaluation. *Anxiety, Stress & Coping*, *25*(2), 167-182. https://doi.org/10.1080/10615806.2011.569709

Schmitz, K. E., Hovell, M. F., Nichols, J. F., Irvin, V. L., Keating, K., Simon, G. M., Gehrman, C., & Jones, K. L. (2004). A validation study of early adolescents' pubertal self-assessments. *The Journal of Early Adolescence*, *24*(4), 357-384. https://doi.org/10.1177/0272431604268531

Schneier, F. R., Blanco, C., Antia, S. X., & Liebowitz, M. R. (2002). The social anxiety spectrum. *Psychiatric Clinics of North America*, *25*(4), 757-774. https://doi.org/10.1016/s0193-953x(02)00018-7

Schneier, F. R., Blanco, C., Antia, S. X., & Liebowitz, M. R. (2002). The social anxiety spectrum. *Psychiatric Clinics of North America*, *25*(4), 757-774. https://doi.org/10.1016/s0193-953x(02)00018-7

Shackman, A. J., & Fox, A. S. (2016). Contributions of the central extended amygdala to fear and anxiety. *Journal of Neuroscience*, *36*(31), 8050-8063. https://doi.org/10.1523/jneurosci.0982-16.2016

Sheehan, D. V., Lecrubier, Y., Sheehan, K. H., Amorim, P., Janavs, J., Weiller, E., … Dunbar, G. C. (1998). The Mini-International Neuropsychiatric Interview (M.I.N.I.): the development and validation of a structured diagnostic psychiatric interview for DSM-IV and ICD-10. The Journal of Clinical Psychiatry, 59 Suppl 20, 22-33;quiz 34-57.

Sheehan, D. V., Sheehan, K. H., Shytle, R. D., Janavs, J., Bannon, Y., Rogers, J. E., Milo, K. M., Stock, S. L., & Wilkinson, B. (2010). Reliability and validity of the mini international neuropsychiatric interview for children and adolescents (MINI-KID). *The Journal of Clinical Psychiatry*, *71*(03), 313-326. https://doi.org/10.4088/jcp.09m05305whi

Shirtcliff, E. A., Dahl, R. E., & Pollak, S. D. (2009). Pubertal development: Correspondence between hormonal and physical development. *Child Development*, *80*(2), 327-337. https://doi.org/10.1111/j.1467-8624.2009.01263.x

Smith, S. M., & Nichols, T. E. (2009). Threshold-free cluster enhancement: addressing problems of smoothing, threshold dependence and localisation in cluster inference. Neuroimage, 44(1), 83-98.

Somerville, L. H., Wagner, D. D., Wig, G. S., Moran, J. M., Whalen, P. J., & Kelley, W. M. (2013). Interactions between transient and sustained neural signals support the generation and regulation of anxious emotion. *Cerebral Cortex*, *23*(1), 49-60. https://doi.org/10.1093/cercor/bhr373

Somerville, L. H., Whalen, P. J., & Kelley, W. M. (2010). Human bed nucleus of the stria Terminalis indexes Hypervigilant threat monitoring. *Biological Psychiatry*, *68*(5), 416-424. https://doi.org/10.1016/j.biopsych.2010.04.002

Stein, D. J., Lim, C. C. W., Roest, A. M., de Jonge, P., Aguilar-Gaxiola, S., Al-Hamzawi, A., … WHO World Mental Health Survey Collaborators. (2017). The cross-national epidemiology of social anxiety disorder: Data from the World Mental Health Survey Initiative. BMC Medicine, 15(1), 143. https://doi.org/10.1186/s12916-017-0889-2

Stevens, F. L., Hurley, R. A., & Taber, K. H. (2011). Anterior Cingulate cortex: Unique role in cognition and emotion. *The Journal of Neuropsychiatry and Clinical Neurosciences*, *23*(2), 121-125. https://doi.org/10.1176/jnp.23.2.jnp121

Straube, T., Mentzel, H., & Miltner, W. H. (2005). Common and distinct brain activation to threat and safety signals in social phobia. *Neuropsychobiology*, *52*(3), 163-168. https://doi.org/10.1159/000087987

Sylvers, P., Lilienfeld, S. O., & LaPrairie, J. L. (2011). Differences between trait fear and trait anxiety: Implications for psychopathology. *Clinical Psychology Review*, *31*(1), 122-137. https://doi.org/10.1016/j.cpr.2010.08.004

Theiss, J. D., Ridgewell, C., McHugo, M., Heckers, S., & Blackford, J. U. (2017). Manual segmentation of the human bed nucleus of the stria terminalis using 3 T MRI. *NeuroImage*, *146*, 288-292. https://doi.org/10.1016/j.neuroimage.2016.11.047

Thomas, K. M., Drevets, W. C., Dahl, R. E., Ryan, N. D., Birmaher, B., Eccard, C. H., ... & Casey, B. J. (2001). Amygdala response to fearful faces in anxious and depressed children. *Archives of general psychiatry*, *58*(11), 1057-1063.

Tillfors, M., Furmark, T., Marteinsdottir, I., & Fredrikson, M. (2002). Cerebral blood flow during anticipation of public speaking in social phobia: A PET study. *Biological Psychiatry*, *52*(11), 1113-1119. https://doi.org/10.1016/s0006-3223(02)01396-3

Tillman, R. M., Stockbridge, M. D., Nacewicz, B. M., Torrisi, S., Fox, A. S., Smith, J. F., & Shackman, A. J. (2018). Intrinsic functional connectivity of the central extended amygdala. *Human Brain Mapping*, *39*(3), 1291-1312. https://doi.org/10.1002/hbm.23917

Tustison, N. J., Avants, B. B., Cook, P. A., & Gee, J. C. (2010). N4ITK: Improved N3 bias correction with robust B-spline approximation. *2010 IEEE International Symposium on Biomedical Imaging: From Nano to Macro*. https://doi.org/10.1109/isbi.2010.5490078

Tyszka, J. M., & Pauli, W. M. (2016). In vivo delineation of subdivisions of the human amygdaloid complex in a high-resolution group template. Human brain mapping, 37(11), 3979–3998. https://doi.org/10.1002/hbm.23289

Vijayakumar, N., Pfeifer, J. H., Flournoy, J. C., Hernandez, L. M., & Dapretto, M. (2019). Affective reactivity during adolescence: Associations with age, puberty and testosterone. *Cortex*, *117*, 336-350.

Williams, L. E., Oler, J. A., Fox, A. S., McFarlin, D. R., Rogers, G. M., Jesson, M. A., Davidson, R. J., Pine, D. S., & Kalin, N. H. (2015). Fear of the unknown: Uncertain anticipation reveals amygdala alterations in childhood anxiety disorders. *Neuropsychopharmacology*, *40*(6), 1428-1435. https://doi.org/10.1038/npp.2014.328

Worsley, K. J., Marrett, S., Neelin, P., Vandal, A. C., Friston, K. J., & Evans, A. C. (1996). A unified statistical approach for determining significant signals in images of cerebral activation. Human brain mapping, 4(1), 58-73.

Wright, E. C., Hostinar, C. E., & Trainor, B. C. (2020). Anxious to see you: Neuroendocrine mechanisms of social vigilance and anxiety during adolescence. *European Journal of Neuroscience*, *52*(1), 2516-2529.

Yassa, M. A., Hazlett, R. L., Stark, C. E., & Hoehn-Saric, R. (2012). Functional MRI of the amygdala and bed nucleus of the stria terminalis during conditions of uncertainty in generalized anxiety disorder. *Journal of Psychiatric Research*, *46*(8), 1045-1052. https://doi.org/10.1016/j.jpsychires.2012.04.013

Yilmazer-Hanke, D. M. (2012). Amygdala. *The Human Nervous System*, 759-834. https://doi.org/10.1016/b978-0-12-374236-0.10022-7

Yoo, T. S., Ackerman, M. J., Lorensen, W. E., Schroeder, W., Chalana, V., Aylward, S., ... & Whitaker, R. (2002). Engineering and algorithm design for an image processing API: a technical report on ITK-the insight toolkit. Studies in health technology and informatics, 586-592.

Zacharek, S. J., Kribakaran, S., Kitt, E. R., & Gee, D. G. (2021). Leveraging Big Data to Map Neurodevelopmental Trajectories in Pediatric Anxiety. *Developmental Cognitive Neuroscience*, 100974.

Zhang, Y., Brady, M., & Smith, S. (2001). Segmentation of brain MR images through a hidden Markov random field model and the expectation-maximization algorithm. *IEEE Transactions on Medical Imaging*, *20*(1), 45-57. https://doi.org/10.1109/42.906424